UNIVERSITY OF CALIFORNIA, SAN DIEGO

The impact of the unfolded protein response on human neurons carrying the familial Alzheimer's disease PSEN1-deltaE9 mutation

A Thesis submitted in partial satisfaction of the requirements
for the degree Master of Science

in

Biology

by

Andrew Chen

Committee in Charge:

Professor Lawrence Goldstein, Chair
Professor Shelley Halpain, Co-Chair
Professor Maho Niwa Rosen

2017

The Thesis of Andrew Chen is approved, and it is acceptable in quality and form for publication on microfilm and electronically:

Co-Chair

Chair

University of California, San Diego

2017

DEDICATION

I dedicate this thesis to my mother, for instilling in me my love of science and biology, and for her unconditional love and support.

TABLE OF CONTENTS

LIST OF FIGURES

LIST OF TABLES

ACKNOWLEDGEMENTS

First and foremost, I would like to express my deepest gratitude to Dr. Larry Goldstein for accepting me into his lab and participate in one of the greatest learning experiences of my life. I have learned so much during my time here, about Alzheimer's disease, about the trials and tribulations of research, and about myself.

I would also like to thank Dr. Shelley Halpain and Dr. Maho Niwa Rosen for taking time out of their schedules serving on my committee.

Next I want to thank my mentor, Dr. Angels Almenar-Queralt, for her continued guidance and support during my time here. Her mentorship, both in lab and in life have played a pivotal role in my growth as a student researcher and as a person out of lab. Next I would like to all the members of the Goldstein lab, past and present, for their amazing positivity, quirkiness, and endless energy, day in and day out. To be surrounded by such intelligent and kind people for two years was truly a blessing, and made my time here even more unforgettable. I would especially like to thank Dr. Rodrigo dos Santos Chaves for the random check-ups with how my research was progressing, and for engaging in random, late-night discussions during tissue culture; Cheryl Herrera for helping me get situated in the lab when I first joined; Dr. Paulina Ordonez and Dr. Bridget Kohlnhofer for their helpfulness and energy to keep things exciting. I would also like to extend my thanks to Dr. Ella Tour for her assistance in the preparation of this written thesis.

I would like to thank all my friends and family for their continued support and encouragement. Their continued support and positivity kept me going as I pursued my graduate degree.

Finally, I would like to thank my mom, for her unconditional love and support throughout my life, for instilling in me my love of science, and for being the greatest role model I have ever had. Nothing that I have accomplished up to today and in the future, would be possible without her.

ABSTRACT OF THESIS

The impact of the unfolded protein response on human neurons carrying the familial Alzheimer's disease PSEN1-deltaE9 mutation

by

Andrew Chen

Master of Science in Biology

University of California, San Diego, 2017

Professor Lawrence Goldstein, Chair
Professor Shelley Halpain, Co-Chair

Alzheimer’s disease (AD) is characterized by extensive cell death and accumulation of misfolded proteins in the brain, which consist of amyloid beta (Aβ) plaques and hyperphosphorylated tau neurofibrillary tangles (NFTs). We sought to determine the effects of endoplasmic reticulum (ER) stress on classical AD characteristics in neurons and neural stem cells (NSCs). We used isogenic human

induced pluripotent stem cell (hiPSC)-derived neurons and NSCs that were genetically modified with the presenilin 1 exon 9 deletion (PS1-ΔE9) mutation. We found that after two days, tunicamycin induced cell death in the PS1-ΔE9 neurons, but not wild type neurons; treatment for five days with thapsigargin, however, induced more cell death in wild type neurons than PS1-ΔE9 neurons.

While previous studies have suggested connections between ER stress, Aβ, and phosphorylated tau (P-tau), results have remained controversial. To measure the effects of ER stress on Aβ42/Aβ40 and P-tau/T-tau (total tau) ratios, we treated neurons with tunicamycin or thapsigargin for two or five days. We observed no change in Aβ42/Aβ40 ratio with tunicamycin or thapsigargin, but observed a dose- and time-dependent reduction in overall Aβ42 and Aβ40 levels. P-tau/T-tau ratio was decreased in PS1-ΔE9, but not wild type neurons in response to both tunicamycin and thapsigargin at 2 days. However, after 5 days of treatment we observed reduced P-tau/T-tau ratio in response to tunicamycin only in wild type and PS1-ΔE9 neurons. The results presented in this study show that the PS1-ΔE9 mutation sensitizes and confers resistance to neurons in response to different ER stressors, and suggest that ER stress may rescue AD phenotypes.

INTRODUCTION

Alzheimer's Disease

Alzheimer's Disease (AD) is the most common cause of dementia and is a fatal, progressive neurodegenerative disease (Barnes and Yaffe, 2011). It is characterized by abnormal accumulation of misfolded proteins in the form of amyloid plaques or neurofibrillary tangles (Shepherd *et al*., 2009; Taylor *et al*., 2002). There are two forms of AD: sporadic AD (SAD) and familial AD (FAD). FAD occurs in patients as young as 40 or 50 years of age, and makes up just 1-5% of all AD cases(Alzheimer's Association; Strobel). SAD is the most common form of Alzheimer's and typically occurs in adults over 65 years old; 95-99% of all AD cases are of sporadic origin. Three primary genes have been identified as causative of FAD: *amyloid precursor protein (APP)*, *presenilin 1* (*PSEN1*), and *presenilin 2* (*PSEN2*) (Bekris et al., 2010). *PSEN1* codes the presenilin-1 (PS1) protein: one of four core proteins that make up the gamma (γ) secretase complex which cleaves APP, a type 1 transmembrane protein, to generate amyloid-beta (Aβ) protein fragments (Haapasalo and Kovacs, 2011). Aβ peptide fragments that are 40- and 42-amino acids long are more involved in AD progression, with the latter being more prone to aggregation and forming the characteristic amyloid plaques (Taylor *et al*., 2002).

Another key protein in AD pathogenesis is the microtubule-associated protein (MAP) tau. Tau protein is the major component of MAPs in axons and is critical for stabilizing microtubules and mediating axonal transport (Rodríguez-Martín et al., 2013; Weingarten et al., 1975). Under pathological conditions tau aggregates into paired helical fragments (PHFs) and neurofibrillary tangles (NFTs) (Kosik et al., 1986). Hyperphosphorylation of tau (pTau) has been suggested to increase aggregation and contribute to disease progression (Grundke-Iqbal et al., 1986).

Endoplasmic Reticulum Stress and the Unfolded Protein Response in Alzheimer's disease

The ER functions as the primary site for protein synthesis, folding, and calcium storage. Disruptions in ER calcium levels, chaperone protein function, and ER-associated degradation (ERAD) pathways can result in a condition called ER stress (Cornejo and Hetz, 2013). To relieve this stress, the ER initiates a series of signal transduction cascades to reduce translation, increase transcription of chaperone proteins, and target misfolded proteins for degradation (Cornejo and Hetz, 2013; Pereira, 2013). These signal cascades and cellular functions are collectively called the unfolded protein response (UPR) (Cornejo and Hetz, 2013; Forman et al., 2003; Merksamer and Papa, 2010; Naidoo and Brown, 2012; Pereira, 2013; Walter and Ron, 2011). Chronic or irreparable ER stress will result in activation of pro-apoptotic factors in an effort to eliminate damaged cells (Jäger et al., 2012; Katayama et al., 2004; Tabas and Ron, 2011).

There are three specialized ER stress-sensing molecules involved in the human UPR pathway: Inositol-required enzyme 1 α (IRE1α), protein kinase RNA-like ER kinase (PERK), and activating transcription factor 6 (ATF6). Under normal conditions, the three sensors are inactivated due to binding of the ER chaperone binding immunoglobulin protein (BiP/glucose-related protein 78—GRP78), which is encoded by the *HSPA5* gene.(Pereira, 2013). Inducing ER stress causes BiP to be released from these sensors, activating them (Figure 1) (Pereira, 2013; Plácido et al., 2014). BiP is a member of the heat shock protein 70 (HSP70) family and is involved in several ER functions, such as folding of newly synthesized proteins and binding to misfolded proteins to prevent protein aggregation (Gething, 1999).

Activating IRE1α leads to specific degradation of mRNAs that encode proteins with abnormal folding and catalyzes the splicing of a 26 base-pair intron from mRNA encoding the transcription factor X-box binding protein 1 (XBP1). This causes a reading frame shift, resulting in the expression of the spliced form which is a potent transcription activator that upregulates genes encoding proteins that enhance protein folding and targets misfolded proteins for degradation (Cornejo and Hetz, 2013; Lin et al., 2008; Pereira, 2013). IRE1α also activates downstream modulators that induce cellular apoptosis (Lin et al., 2008).

PERK activation attenuates protein synthesis by phosphorylating eukaryotic translation initiator factor 2α (eIF2α). Decreasing protein synthesis is a mechanism to reduce protein load in the ER to help alleviate ER stress. However, phosphorylating eIF2α paradoxically increases translation of activating transcription factor 4 (ATF4). ATF4 activation causes increased translation of ER chaperones in an effort to alleviate ER stress; ATF4 also upregulates translation of the transcription factor CCAAT/enhancer binding protein homologous protein (CHOP) that promotes apoptosis (Lin et al., 2008). Inducing PERK *in vitro* has been shown to attenuate Aβ-mediated ER stress (Lee et al., 2010).

Activation of ATF6 causes its translocation to the Golgi, where it is cleaved by site-1 protease and site-2 protease (Cornejo and Hetz, 2013; Lin et al., 2008). The active fragment is released into the cytosol where it is targeted the nucleus where it activates transcription of ER chaperones, ERAD-related genes, and genes for organelle biogenesis (Pereira, 2013).

As mentioned earlier, chronic or irreparable ER stress activates apoptosis. One mediator is the activation of CHOP, which downregulates anti-apoptotic genes and upregulates pro-apoptotic genes leading to cell death (Jäger *et al*., 2012; Tabas and Ron, 2011). Previous studies have shown evidence of increased levels of ER stress markers in postmortem primary brain tissue of AD patients (Hoozemans et al., 2005, 2009), again suggesting that Aβ and ER stress are linked.

The relationship between presenilin and ER stress in Alzheimer's disease is unclear

One hypothesis for the cause of AD is the amyloid cascade hypothesis, which is based on APP processing. APP can be cleaved through two pathways: the first involves sequential cleavage of APP via α-secretase and γ-secretase to generate α C-terminal fragments (CTFs) and a p53 fragment; this pathway is generally considered the non-amyloidogenic pathway. The second, which is called the amyloidogenic pathway, involves sequential cleavage of APP by β-secretase and γ-secretase, resulting in the production of Aβ fragments of various sizes, the relevant ones being 40-42 amino acids in length (Hardy and Allsop, 1991; Hardy and Higgins, 1992). Over 100 pathogenic PS1 mutations have been characterized in FAD, and these mutations account for the largest proportion of FAD causes; these mutations typically alter the ratio of Aβ42 to Aβ40 in the cell (Kelleher and Shen, 2017; Sun et al., 2017). Altering the ratio of Aβ42 to Aβ40 has been hypothesized as a causative agent for FAD (Scheuner *et al*., 1996). Additionally, introducing exogenous Aβ42 to *in vitro* cultures was shown to induce ER stress and activate the UPR by observing increases in *BiP* and *CHOP* mRNA levels (Lee et al., 2010).

There has been continual debate regarding FAD PS1 mutations and whether they disrupt the ability of neurons to activate the UPR. Niwa et al., 1999 used HeLa cells to demonstrate that PS1 is required for proper IRE1α localization upon activation of the UPR. They also showed that knocking out PS1 in cells compromises UPR function. Katayama et al., 1999 also showed a connection between PS1 and IRE1α function. In their experiments, they discovered that FAD PS1 mutations reduce the efficacy of the UPR signaling pathway in neuroblastoma cells transfected with wild type PS1 and FAD-related PS1 mutations. The same authors found similar results in a second paper as well (Katayama et al., 2001). However, other groups found different results, specifically that fibroblasts obtained from patients bearing a PS1 mutation have a normal UPR (Piccini et al., 2004a), or that upregulation of *BiP* and *CHOP* mRNA in PS1 knockout mouse embryonic fibroblasts and neuroblastoma cells is independent of presenilin expression (Sato et al., 2000).

Involvement of ER stress in tau phosphorylation in Alzheimer's disease

The other key protein involved in AD, tau, is a microtubule-associated protein that promotes the stability of microtubules (Weingarten et al., 1975). Under AD conditions, tau phosphorylation increases, compromising its function resulting in toxic tau aggregation and breakdown of microtubules (Alonso et al., 1994). Hyperphosphorylation of tau is related to the activity of kinases such as glycogen synthase kinase -3 beta (GSK-3β), which has been shown to be activated in response to ER stress caused by thapsigargin, an inhibitor of ER Ca^{2+}-ATPase (Song et al., 2002). GSK-3β was also shown to be activated in response to Aβ oligomer-induced ER Ca^{2+} release, resulting in increases in tau phosphorylation (Resende et al., 2008). Other studies

describing mutations in the *PSEN1* gene have shown associations between different *PSEN1* mutations and changing tau and pTau levels (Dong et al., 2017; Luedecke et al., 2014).

Using hiPSC-derived NSCs and neurons to study ER stress in Alzheimer's disease

Mouse models overexpressing *APP* and/or *PSEN1* genes implicated in FAD are powerful tools that allow researchers to study the impacts of Aβ aggregation on memory and behavior that cannot be seen *in vitro*. Although many such models develop relevant AD-related Aβ pathology such as age-dependent cognitive impairment and memory deficits (Janus et al., 2000), challenges have arisen when attempting to determine the relative contributions of Aβ, APP, and other APP metabolites to AD pathology seen in mouse models. Furthermore, many of these mouse models that overexpress *APP* and/or *PSEN1* do not exhibit symptoms of other pathological features of AD, including neuronal death and the presence and accumulation of neurofibrillary tangles (Drummond and Wisniewski, 2017). The presence of *APP* and/or *PSEN1* overexpression in mice does not guarantee AD-associated neuropathology either (Drummond and Wisniewski, 2017; Kim et al., 2013). While transgenic mice have been generated to express human tau, tangle formation is not observed unless the mice contain mutations associated with frontotemporal lobar degeneration (FTLD) (Drummond and Wisniewski, 2017). These pose a different limitation in that the FTLD-related mutations are not typically seen in AD pathology in humans.

Using human tissue to study AD bypasses many of the issues that result from species differences. However, it poses other challenges, such as the lack of available, quality post-mortem tissue. The development of human induced pluripotent cells

(hiPSCs) (Takahashi et al., 2007) have circumvented many of the pervious limitations in using human tissue, such as using non-neuronal cell lines transfected or transduced with *APP* or *PSEN1* mutations (Katayama et al., 1999, 2004; Niwa et al., 1999).

In order to study the effects of a representative FAD mutation on cell viability, Aβ 42 levels, and hyperphosphorylated tau levels in response to ER stress, we used isogenic human induced pluripotent stem cell (hiPSC)-derived neural stem cells (NSCs) and neurons reprogrammed from fibroblasts from a healthy human donor (Woodruff et al., 2013). The cell lines had their genomes engineered using TAL effector nuclease (TALENs) technology to introduce an allelic series of mutations in the *PSEN1* gene, referred to as the PS1-ΔE9 (PS1-ΔE9). The specific mutation is caused by a deletion of exon 9 in the *PSEN1* gene, and has been shown to generate an AD phenotype as seen by increases in Aβ42/Aβ40 ratio through increasing Aβ42 and decreasing Aβ42 levels (Woodruff et al., 2013). The PS1-ΔE9 mutation present in our cell lines was shown to act also as a gain of function mutation, resulting in a "super leaky" channel, leading to increased cytosolic Ca^{2+} levels and decreased ER Ca^{2+} levels (Chaves R. S., unpublished). Preliminary results from our lab also showed that chemically inducing ER stress in PS1-ΔE9 NSCs and neurons resulted in different levels of induction of well-known ER stress genes (e.g., *BiP* and *XBP1*; Almenar and Roberts, unpublished data), which suggests that PS1-ΔE9 mutants may be more sensitive to ER stress.

RESULTS

PS1-ΔE9 NSCs may be more sensitive to ER stress-induced cell death

In order to mimic conditions of chronic ER stress and to test its effects on cellular viability, we treated control human induced pluripotent stem cell (hiPSC) -derived neural stem cells (NSCs) with varying concentrations of tunicamycin, an *N*-glycosylation inhibitor, which has been shown to induce ER stress (Dorner et al., 1990). Previous studies typically used tunicamycin concentrations ranging between 1-10 μg/ml for anywhere from a few hours (Oslowski and Urano, 2011; Song et al., 2002) to between 24 and 48 hours (Oslowski and Urano, 2011; Takahashi et al., 2009). However, these studies used non-neuronal cell lines, and so to measure the effects of tunicamycin in our system, we treated control NSCs in a dilution series for 24 and 48hrs. No cell death was observed 24hrs after treatment with tunicamycin (Figure 2A), however after 48hrs cell death was observed in a dose-dependent manner with increasing tunicamycin concentration (Figure 2B). We used staurosporine, a compound that induces apoptosis, as a positive control for cell death and observed a dose-dependent decrease in NSC viability at both 24 and 48hrs post-treatment (Figure 2C-D).

Next, to study how the PS1-ΔE9 mutation affects cellular viability in response to induced ER stress, we treated wild-type (WT/WT), heterozygous mutant (WT/ΔE9), and homozygous mutant (ΔE9/ΔE9) NSCs with varying doses of tunicamycin for 24 or 48hrs (Figure 3). We observed that both the wild-type NSCs—which do not have the PS1-ΔE9 mutation and should behave similarly to the control NSCs from Figure 2— and the WT/ΔE9 NSCs showed no significant decrease in cell viability 24hrs post-treatment (Figure 3A; left and center). However, cell viability was significantly, albeit marginally, decreased in the ΔE9/ΔE9 NSCs (Figure 3A; right). The differences in viability between

genotypes in response to tunicamycin was lost after 48hrs, however, with all cells showing up to 50% reduction in viability (Figure 3B; left, center, right). Our data suggests that the PS1-ΔE9 mutation sensitizes NSCs to ER-stress, increasing their susceptibility to ER stress-induced cell death.

Control neurons do not die after ER stress is induced, but still upregulate ER stress genes

Next, we asked whether we would observe the same effects in NSC-differentiated neurons as we saw in NSCs. We differentiated the above control NSCs for three weeks before replating them at uniform density onto a 96-well plate. After waiting two weeks to let the replated neurons recover, we treated neurons with varying doses of tunicamycin for 48hrs, and observed no significant differences in neuron viability, even at a higher concentration of tunicamycin than what was used in NSCs (Figure 4A). However, we did see a downward trend in neuron viability as tunicamycin concentration increased. Staurosporine was used as a positive control for cell death again, and we observed a dose-dependent decrease in cell viability (Figure 4B).

Because no neuron death was observed, we asked whether the neurons were responding to tunicamycin and generating an ER stress response. We measured changes in mRNA levels of two different ER stress genes: *BiP* and spliced *XBP1*. As stated earlier, under ER stress conditions, BiP dissociates from IRE1α, which activates it causing it to splice a 26 base-pair intron from *XBP1* mRNA to generate its spliced form (Figure 1), which is a potent transcription factor that activates many downstream UPR pathways. BiP, being a chaperone protein, will bind to misfolded proteins and is sequestered into complexes with those proteins. The eventual decrease of free BiP may

be the signal that induces increased transcription of ER stress genes (Gething, 1999). After the neurons were treated with tunicamycin for 48hrs, RT-qPCR was performed to measure the relative levels of *BiP* and spliced *XBP1* mRNA. We observed that *BiP* mRNA increased nearly 20-fold (Figure 5A), and spliced *XBP1* mRNA increased by 10- to 20-fold (Figure 5B) with tunicamycin treatment. Taken together, these results show that neurons can initiate the UPR after ER stress is induced by tunicamycin, without inducing cell death.

PS1-ΔE9 neurons differ in their response to induced ER stress compared to controls

Next, we wanted to determine whether neuron viability is reduced by ER stress in neurons expressing the PS1-ΔE9 mutation. To do so, we treated one wild-type control and two independently-generated PS1-ΔE9 mutant neuronal lines for two days or five days with various doses of tunicamycin and measured cellular viability and changes in expression of three ER stress genes: *BiP*, spliced *XBP1*, and *CHOP*. We found that wild-type neurons showed no significant decrease in viability (Figure 6A, left) and significant reductions in viability in both PS1-ΔE9 mutants after two days of tunicamycin treatment. After five days of tunicamycin treatment these differences were lost, and we saw dose-dependent decreases in viability in wild-type and PS1-ΔE9 neurons (Figure 6B). To rule out the possibility that our vehicle treatment was negatively affecting our cells, we mock treated our neurons with only media or with just the vehicle for two and five days. We observed no difference in viability with the vehicle compared to the untreated condition (Figure 6A, untreated; 6C). One hypothesis we had for the different responses to cell viability after treating the cells for two days was that the PS1-ΔE9 mutants may have lower basal viability than the wild-type control. To address this, we counted the cells

using trypan blue on an automated cell counter every time the cells were replated and recorded the percent of viable cells present. We found no significant difference in the basal viability across all three lines (Figure 6D).

After observing a slight difference in viability between PS1-ΔE9 neurons and wild-type neurons after tunicamycin treatment, we asked whether we would observe the same results by using a different ER stress inducer with a different mechanism of action. We chose to use thapsigargin, which induces ER stress by inhibiting SERCA and results in elevated cytosolic Ca^{2+} levels. We treated neurons with thapsigargin for two or five days before measuring cell viability and saw no decrease in cell viability in wild-type neurons (Figure 7A, left) and only slight reduction of cell viability in one of the PS1-ΔE9 mutants (Figure 7A, center) after two days of thapsigargin treatment. Interestingly, after five days the thapsigargin induced approximately 25% decrease in viability in wild-type neurons (Figure 7B; left), whereas it had little to no effect on the PS1-ΔE9 neurons (Figure 7B; center and right).

To address our initial hypothesis that PS1-ΔE9 neurons would have a constitutively activated UPR, we also measured basal expression of ER stress-related genes after treatment with only the drug vehicle: DMSO. We found that control and PS1-ΔE9 neurons have similar basal expression of *BiP* (Figure 8A; left) but have different levels of spliced *XBP1* and *CHOP* (Figure 8A; center and right). Upon treatment with tunicamycin for two days we found that the three ER stress genes showed elevated expression levels compared to the vehicle treatment (Figure 8B). However, wild-type and PS1-ΔE9 neurons exhibited similarly elevated levels of *BiP* and spliced *XBP1* expression when treated with tunicamycin (Figure 8B; left, center), except the ΔE9/ΔE9-1 mutant

line showed significantly elevated levels of *CHOP* expression compared to both wild-type and the ΔE9/ΔE9-2 mutant, which was not significantly different compared to wild-type (Figure 8B; right). When we treated the neurons with thapsigargin, wild-type neurons showed a nearly three-fold increase in *BiP* expression compared to both PS1-ΔE9 mutants (Figure 8C; left); spliced *XBP1* was significantly different between wild-type and only one of the PS1-ΔE9 neurons (Figure 8C, middle). Additionally, *CHOP* expression was higher in wild-type neurons compared to both PS1-ΔE9 mutants (Figure 8C; right). Our results here suggest the PS1-ΔE9 mutation may sensitize neurons to tunicamycin-induced ER stress while conferring resistance to thapsigargin-induced ER stress. Additionally, our results show no consistent elevation or suppression of expression of three ER stress genes, suggesting that the PS1-ΔE9 does not alter the neurons' ability to activate the ER stress response after insult.

Effects of induced ER stress on secreted Aβ42 and Aβ40 levels

Previous studies on Aβ and ER stress have shown connections between the two, with evidence for oligomeric forms of Aβ42 activating the ER stress response (Lee et al., 2010), along with Aβ accumulation associated with inducing ER stress (as reviewed by Placido et al., 2014). The PS1-ΔE9 mutation was previously shown to increase the Aβ42/40 ratio by increasing Aβ42 and decreasing Aβ40 (Woodruff et al., 2013). Because the primary function of the ER stress response and the UPR is to alleviate stress from misfolded or accumulated proteins, we asked whether inducing ER stress would increase or decrease the elevated Aβ42/Aβ40 ratio observed in the PS1-ΔE9 neurons. We treated replated neurons with varying doses of tunicamycin for two or five days, and collected the media to measure soluble Aβ42 and Aβ40. We observed no significant change in the

Aβ42/Aβ40 ratio after treating the wild-type and PS1-ΔE9 mutants with tunicamycin for two days (Figure 9A). When looking at Aβ42 and Aβ40 levels individually, we noticed that both Aβ42 and Aβ40 exhibited a downward trend as tunicamycin dose increased (Figure 9B, C) across the three neuron lines. Interestingly, we saw significant decreases in only Aβ40 levels with 10 μM tunicamycin treatment in the WT/WT line (Figure 9C, left), along with significant decreases in Aβ42 and Aβ40 levels in only one PS1-ΔE9 mutant (Figure 9B, C; center), but not the other. After treating wild-type and PS1-ΔE9 neurons with tunicamycin for five days we observed no changes to the Aβ42/Aβ40 ratio in wild-type or PS1-ΔE9 neurons (Figure 10A). When we looked at Aβ42 and Aβ40 levels, we saw very significant decreases in Aβ42 and Aβ40 in the wild-type and both PS1-ΔE9 neurons (Figure 10B, C).

Next we wanted to see if we would observe similar effects on Aβ42, Aβ40, or the Aβ42/Aβ40 ratio when we treated neurons with thapsigargin for two or five days. Here we also observed no significant change in the Aβ42/Aβ40 ratio in wild-type or PS1-ΔE9 mutants (Figure 11A). When looking at Aβ42 and Aβ40 levels individually, however, we saw no significant changes in the levels of either Aβ42 and Aβ40 (Figure 11B, C). We did observe a slight downward trend in Aβ42 and Aβ40 levels in the WT/WT and ΔE9/ΔE9-1 lines, but not in the ΔE9/ΔE9-2 line. After five days of thapsigargin treatment, we observed no change in the Aβ42/Aβ40 ratio (Figure 12A). When looking at Aβ42 and Aβ40 individually, however, we saw slight decreases in Aβ42 and Aβ40 in the wild-type line (Figure 12B, C; left) and inconsistent changes in the PS1-ΔE9 mutants (Figure 12B, C; center, right). Overall these results suggest that ER stress, induced by tunicamycin or thapsigargin for two days, does not increase or decrease the Aβ42/Aβ40

ratio in wild-type or PS1-ΔE9 mutant neurons. After five days, however, tunicamycin significantly reduces levels of Aβ42 and Aβ40 in wild-type and PS1-ΔE9 neurons without changing the Aβ42/Aβ40 ratio, while thapsigargin appears to primarily affects wild-type neurons. Our results suggest that inducing ER stress in neurons decreases overall Aβ42 and Aβ40 without affecting Aβ42/Aβ40, regardless of genotype.

Effects of induced ER stress on tau phosphorylation

Next we wanted to determine whether ER stress can affect the P-tau/T-tau ratio. Previous studies have shown involvement of ER stress in hyperphosphorylation of tau (Grundke-Iqbal et al., 1986; Hoozemans et al., 2009), which is the primary protein that forms the neurofibrillary tangles seen in AD. We treated wild-type and PS1-ΔE9 mutant neurons with 1 μM of tunicamycin and 1 μM of thapsigargin for two or five days before measuring total tau (T-tau) and phosphorylated tau (P-tau) in whole cell lysate. We observed no change in the P-tau/T-tau ratio in wild-type neurons after two-day treatment with tunicamycin or thapsigargin (Figure 13A, left). This was due to no observed changes in P-tau (Figure 13B, left) or T-tau (Figure 13C, left). When the PS1-ΔE9 mutants were treated with 1 μM tunicamycin or 1 μM thapsigargin, we observed approximately a 25% decrease in the P-tau/T-tau ratio compared to the vehicle treatment (Figure 13A; center, right). The reason for this decrease, however, differed between the two mutant lines. We observed a significant decrease in P-tau in the ΔE9/ΔE9-1 neurons (Figure 13B, center) after thapsigargin treatment, and a slight decrease after tunicamycin treatment (although not significant). This was accompanied by a slight increase in T-tau after tunicamycin treatment, but no change in T-tau after thapsigargin treatment (Figure 13C, center). In the ΔE9/ΔE9-2 neurons, we observed a slight increase in P-tau after treatment with 1 μM

tunicamycin (Figure 13B, right) along with an almost 50% increase in T-tau after tunicamycin treatment (Figure 13C, right). We observed that thapsigargin-induced ER stress did not change P-tau levels in the ΔE9/ΔE9-2 neurons (Figure 13B, right), but it may have subtly increased T-tau levels (Figure 14C, right), leading to an overall decrease in the P-tau/T-tau ratio.

After we treated wild-type and the PS1-ΔE9 neurons with tunicamycin and thapsigargin for five days, we observed greatly reduced P-tau/T-tau ratios in the wild-type and both PS1-ΔE9 mutants with tunicamycin treatment, but only a significant decrease in P-tau/T-tau ratio with thapsigargin treatment in the wild-type line (Figure 14A). Interestingly, the P-tau/T-tau ratio dropped to approximately the same value in all three cell lines treated with tunicamycin (~0.005). The reduction in the P-tau/T-tau ratio after tunicamycin treatment was primarily due to decreases in P-tau (Figure 14B) whereas T-tau was not significantly affected in the wild-type or PS1-ΔE9 neurons (Figure 14C). These results suggest that long-term induction of ER stress with tunicamycin, not thapsigargin, reduces the P-tau/T-tau ratio by decreasing P-tau levels.

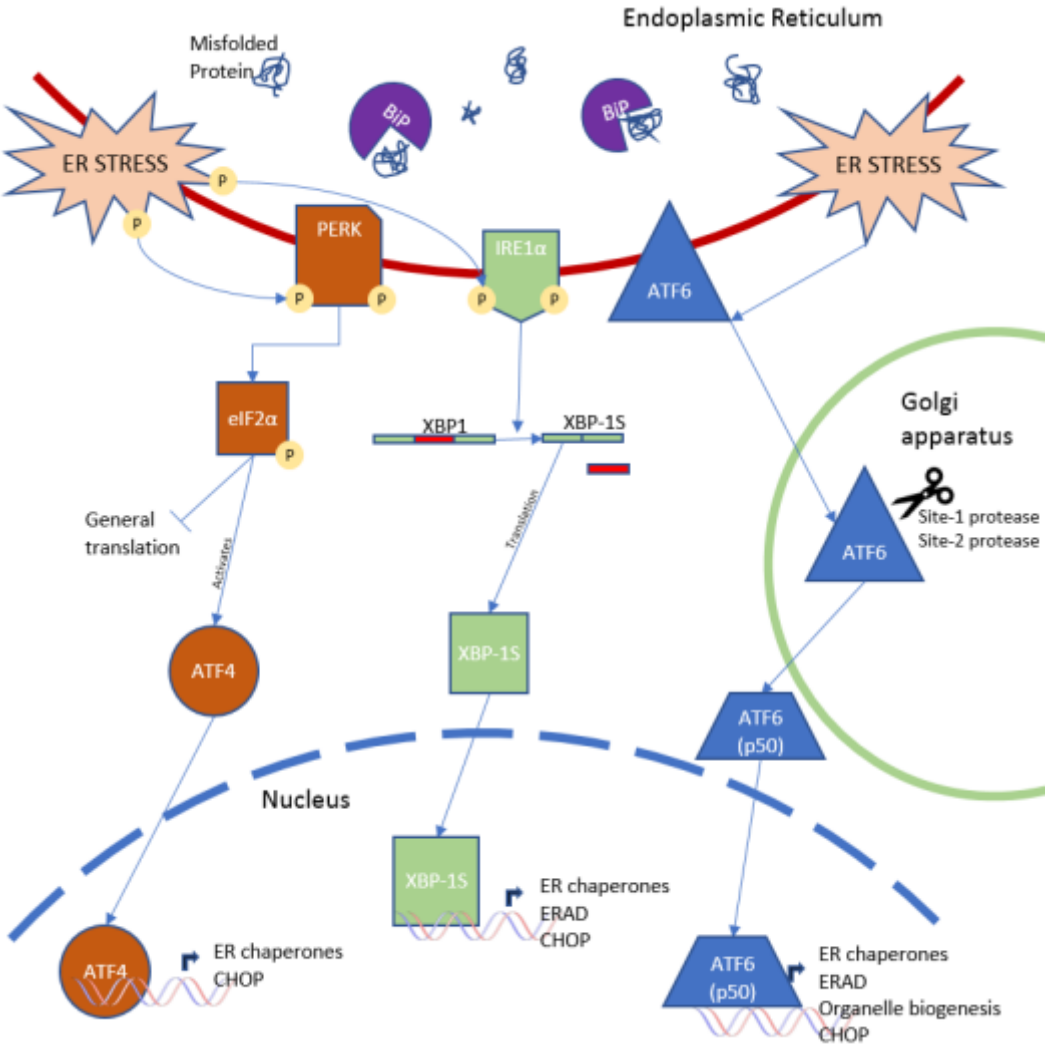

Figure 1. The Unfolded Protein Response. Disruptions in endoplasmic reticulum (ER) homeostasis results in activation of signal cascades associated with the ER stress sensors: protein kinase RNA-like ER kinase (PERK), inositol-requiring enzyme-1alpha (IRE1α), and activating transcription factor 6 (ATF6). Under non-stressed conditions, these three sensors are inactivated through binding with BiP. However, accumulation of misfolded proteins causes BiP to dissociate from the three sensors, which become activated. Active PERK phosphorylates eIF2α which attenuates general translation, resulting in overall decreased protein load in the cell. eIF2α paradoxically increases translation of activating transcription factor 4 (ATF4), which induces transcription of ER chaperones. Activated IRE1α splices a 26-base pair segment of *XBP1* mRNA; this spliced form induces transcription of ER chaperones and ER-associated protein degradation pathway genes. Activated ATF6 migrates to the Golgi apparatus, where it is cleaved by site-1 and site-2 proteases. This cleaved form (ATF6p50) migrates to the nucleus where it upregulates UPR elements. Under conditions of chronic or irreparable ER stress, all three pathways are capable of inducing ER stress-mediated apoptosis by upregulating pro-apoptotic genes such as C/EBP-homologous protein (CHOP).

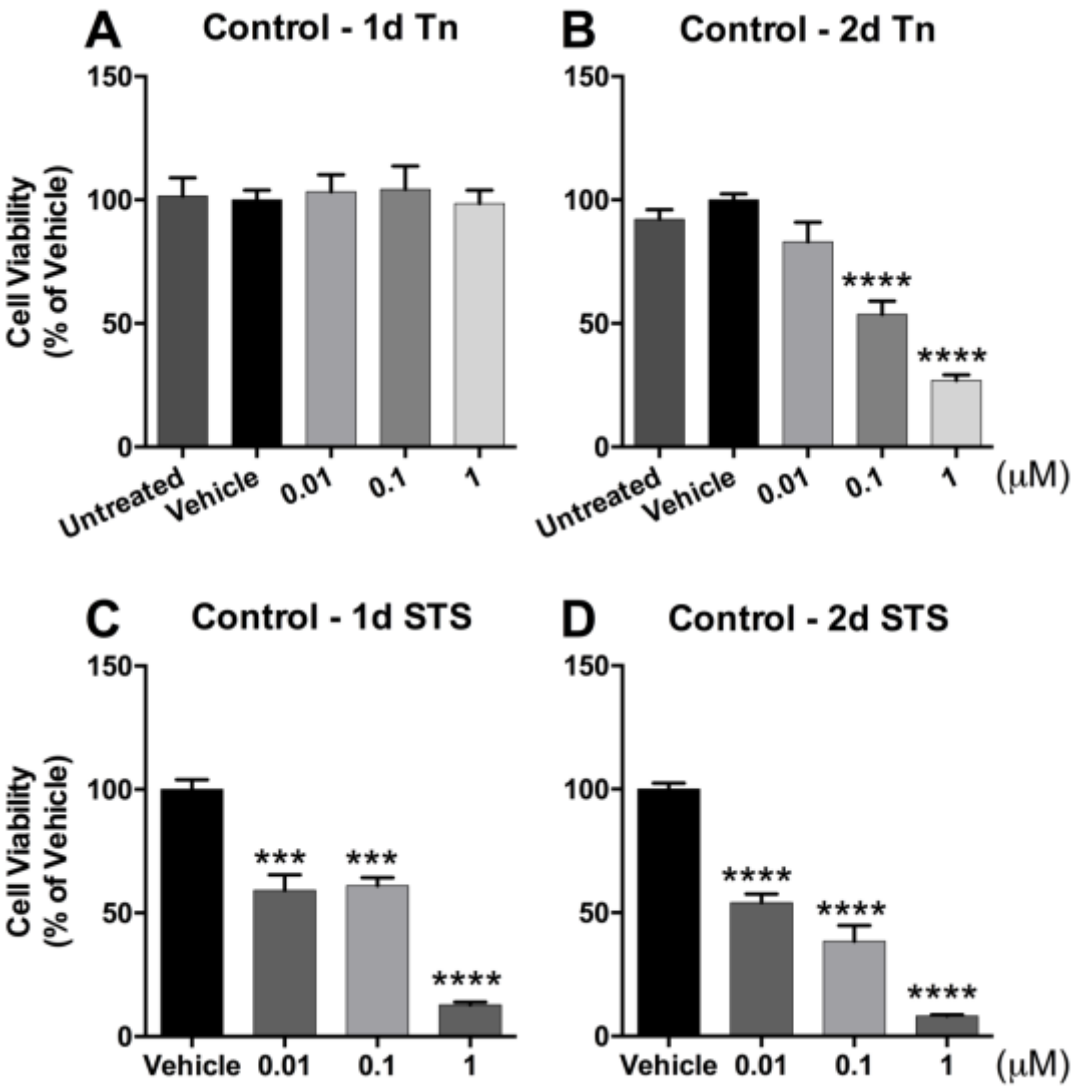

Figure 2. Tunicamycin induces death in a dose- and time-dependent manner in control NSCs. (A-B) Control NSCs were treated with tunicamycin (Tn) at various doses for one or two days. (C-D) Control NSCs were treated with staurosporine (STS) at various doses for one or two days. Bars represent mean of three independent experiments. Error bars represent SEM of three biological replicates per experiment. ****$p < 0.0001$ by One-way ANOVA.

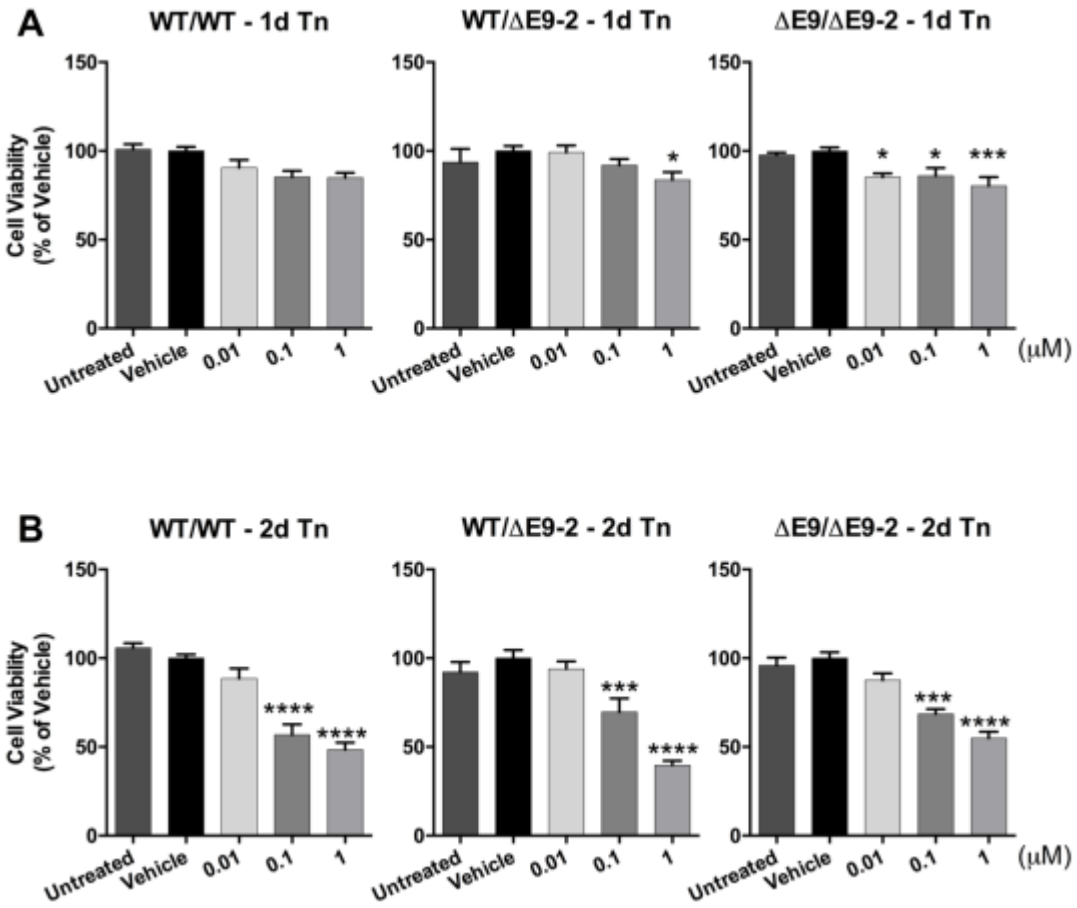

Figure 3. PS1-ΔE9 NSCs differ in viability in response to tunicamycin-induced ER stress. NSCs were treated with the drug vehicle, tunicamycin at varying doses, or mock treated (untreated), for one (A) or two (B) days. Cell viability is expressed as percent viable cells compared to vehicle. Bars represent mean of three independent experiments. Error bars represent SEM of three biological replicates per experiment. ****$p < 0.0001$ by One-way ANOVA.

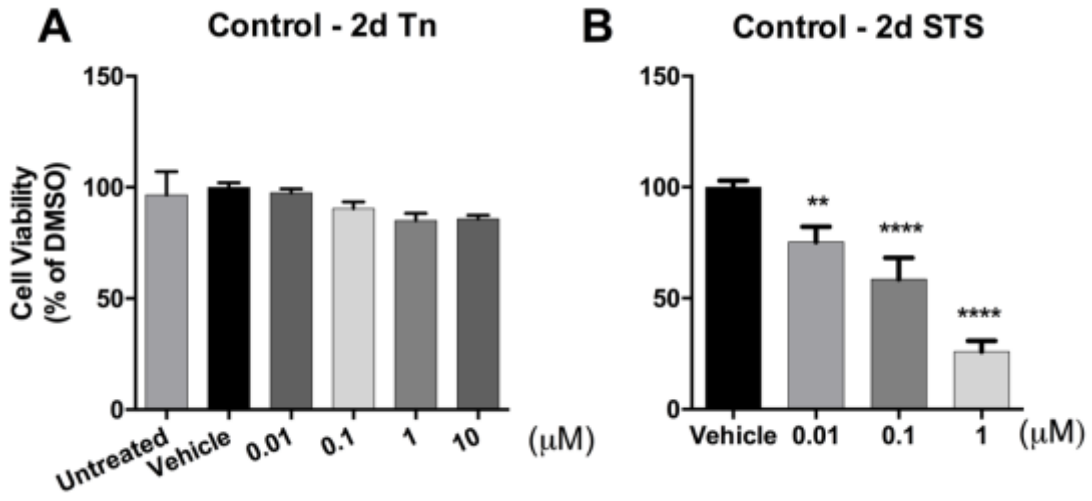

Figure 4. Control neurons are more resilient to tunicamycin-induced ER stress than NSCs. (A) Neurons were treated with tunicamycin (Tn) at varying doses for two days. Bars represent mean of three independent experiments. Error bars represent SEM of three biological replicates per experiment. (B) Control neurons were treated with staurosporine (STS) at varying doses for two days to serve as a positive control for cell death. Bars represent mean of three independent experiments. Error bars represent SEM of three biological replicates per experiment. *p<0.05, **p<0.01, ***p<0.001, ****p < 0.0001 by One-way ANOVA.

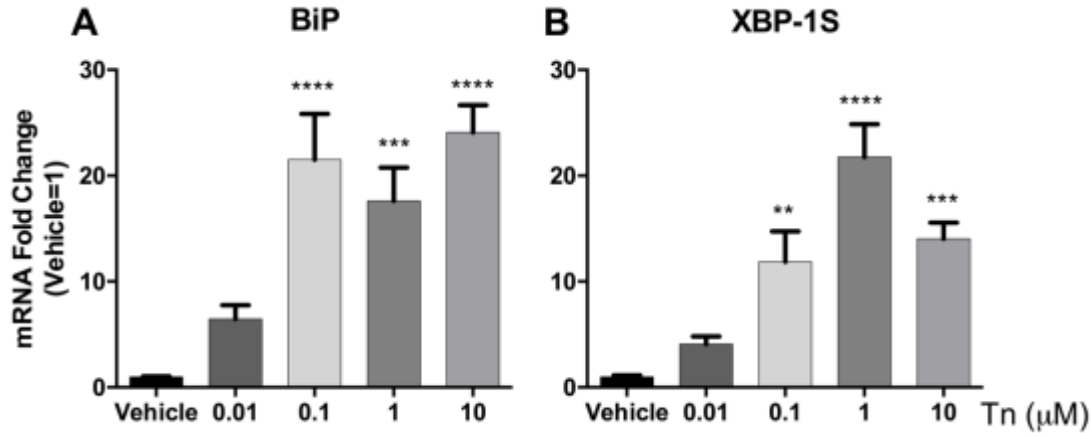

Figure 5. Tunicamycin induces elevated transcription of ER stress genes without reducing cellular viability. Control neurons were treated with varying concentrations of tunicamycin (Tn) for two days. RT-qPCR was done to measure the relative fold change in gene expression. Bars represent the mean from three independent experiments. Error bars represent SEM of three technical replicates per condition. *p<0.05, **p<0.01, ***p<0.001, ****p < 0.0001 by One-way ANOVA.

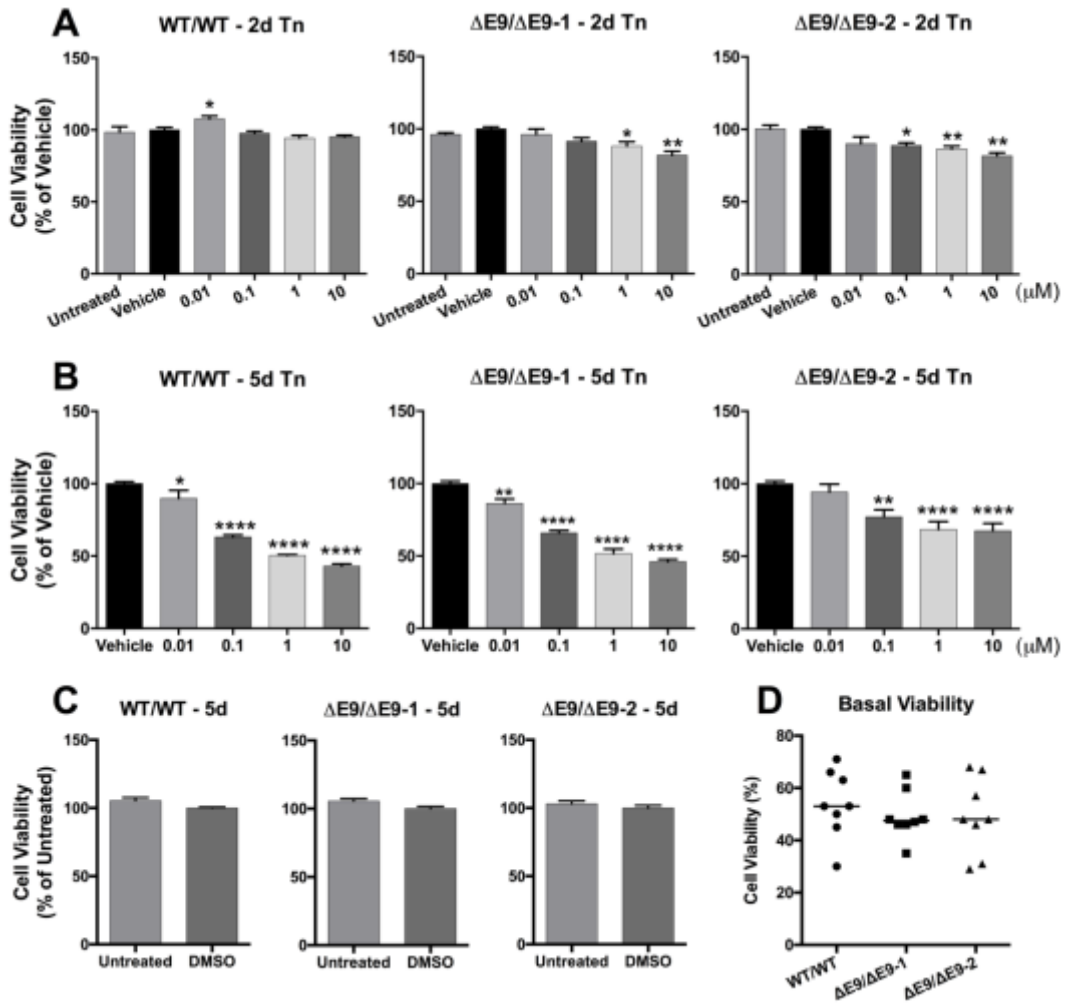

Figure 4. PS1-ΔE9 neurons are marginally more sensitive to ER stress-induced death. (A) Neuron viability measured as percentage of vehicle after treatment with varying concentrations (μM) of tunicamycin (Tn) for two days. Bars represent measurements from three independent experiments per condition. Error bars represent SEM from 9 biological replicates per condition. (B) Neuron viability measured as percentage of vehicle after treatment with varying concentrations (μM) of tunicamycin (Tn) for five days. Bars represent measurements from three independent experiments per condition. Error bars represent SEM from 9 biological replicates per condition. (C) Neuron viability measured as percentage of vehicle after mock treatment (untreated) or vehicle only treatment. Bars represent measurements from one experiment per line. Error bars represent SEM from three biological replicates per condition. (D) Basal neuron viability measured as percent survival after trypan blue count prior to replating. Scatter dot plot represents median percentage of viable cells from three independent experiments. (A-D) Statistics performed using One-way ANOVA. *p<0.05, **p<0.01, ***p<0.001, ****p < 0.0001

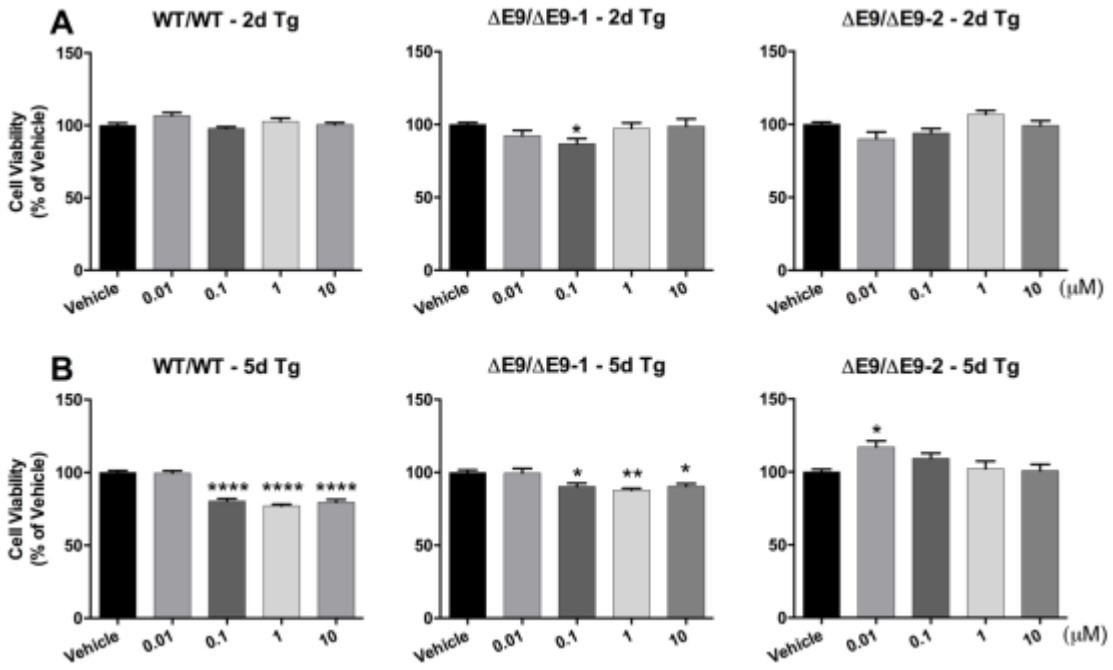

Figure 5. PS1-ΔE9 neurons are less sensitive to thapsigargin-induced ER stress cell death. (A) Neuron viability measured as percentage of vehicle after treatment with varying concentrations of thapsigargin (Tg) for two days. Bars represent measurements from three independent experiments per condition. Error bars represent SEM from 9 biological replicates per condition. Statistics performed using One-way ANOVA. Dashed line = 100% viability. (B) Neuron viability measured as percentage of vehicle after treatment with varying concentrations of thapsigargin (Tg) for five days. Bars represent measurements from three independent experiments per condition. Error bars represent SEM from 9 biological replicates per condition. Statistics performed using One-way ANOVA. Dashed line = 100% viability. *p<0.05, **p<0.01, ***p<0.001, ****p < 0.0001

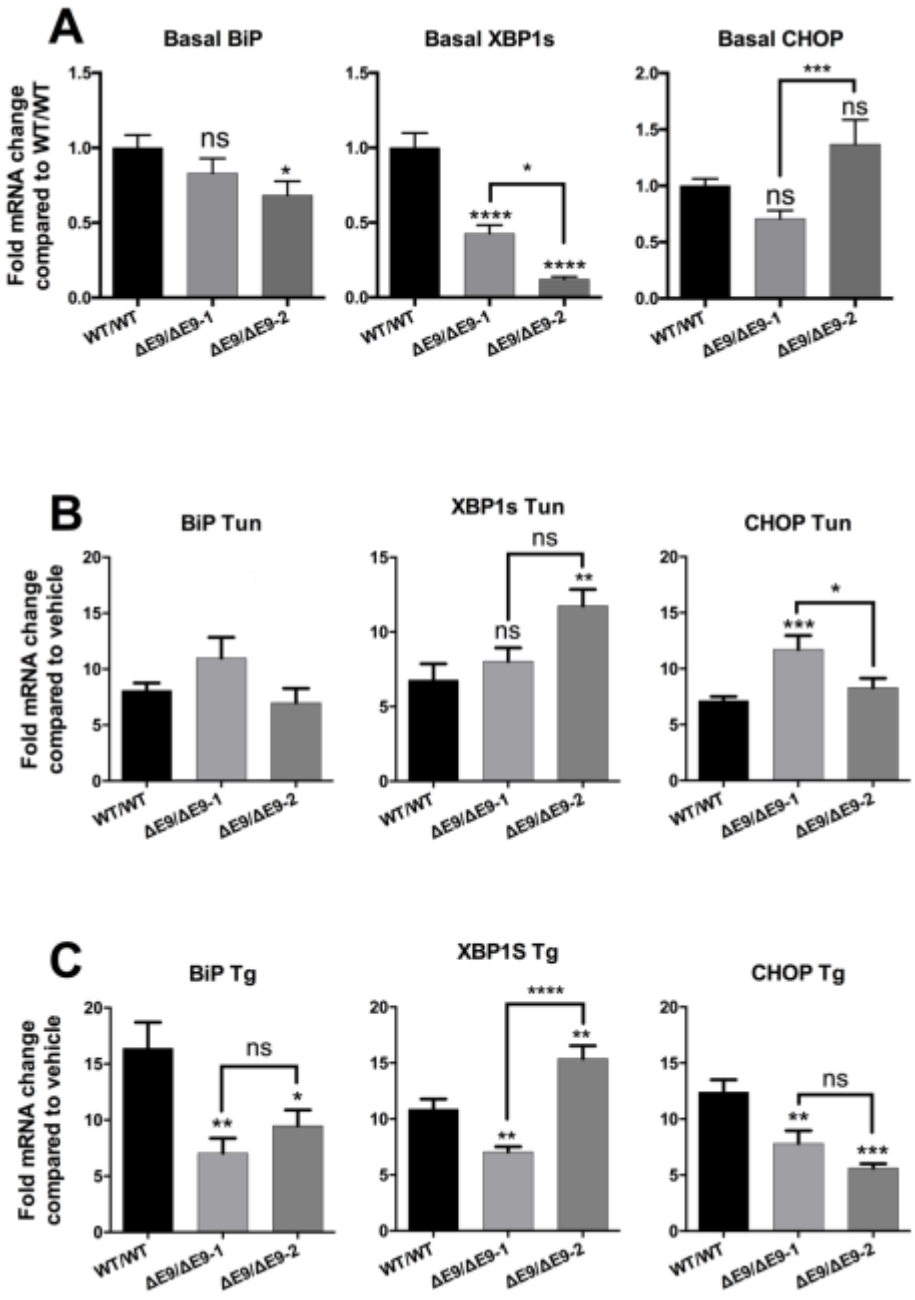

Figure 6. PS1-ΔE9 neurons express different levels of ER stress genes compared to wild-type neurons. Wild-type or PS1-ΔE9 neurons were treated with 1 μM of either tunicamycin (Tn) or thapsigargin (Tg) for two days. RT-qPCR was performed to measure the relative fold change in mRNA. Bars represent the mean fold change of each gene normalized to three house-keeping genes: *RPL17*, *RPL13A*, and *TBP*, and then normalized to vehicle = 1 (not shown) from two independent experiments. Error bars represent SEM from three technical replicates per treatment condition. *p<0.05, **p<0.01, ***p<0.001, ****p < 0.0001 by One-way ANOVA

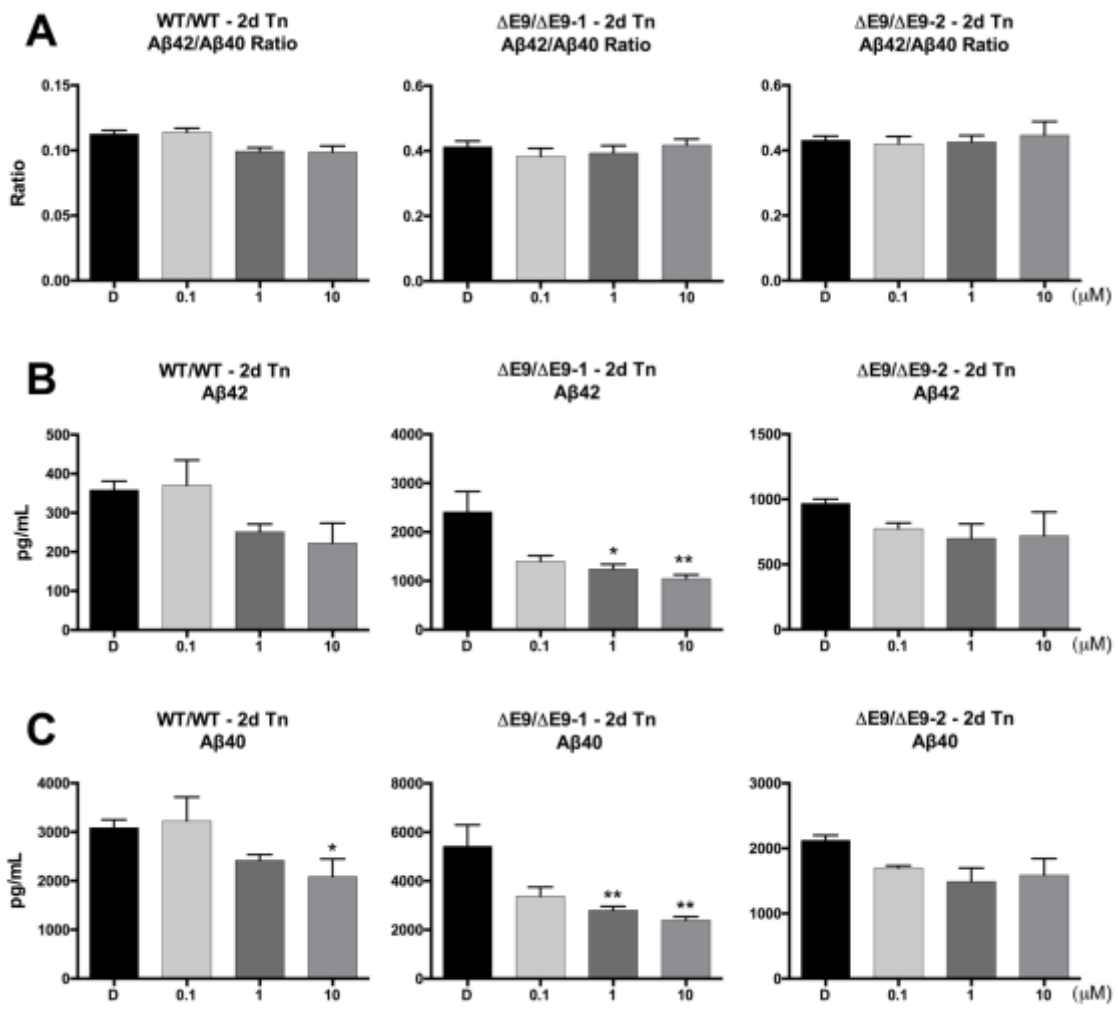

Figure 7. Tunicamycin-induced ER stress does not change the Aβ42/Aβ40 ratio. Secreted Aβ42/Aβ40 ratio (A), Aβ42 (B), and Aβ40 (C) were measured from wild-type and PS1-ΔE9 mutants treated with increasing concentrations of tunicamycin (Tn) for two days. Bars represent measurements from one experiment normalized to total protein concentration. Error bars represent SEM from three biological replicates per experiment. Additional experiments were repeated and showed similar results, but could not normalize to total protein (data not shown). Statistics performed via One-way ANOVA. *p < 0.05, **p<0.01, ***p<0.001, ****p<0.0001.

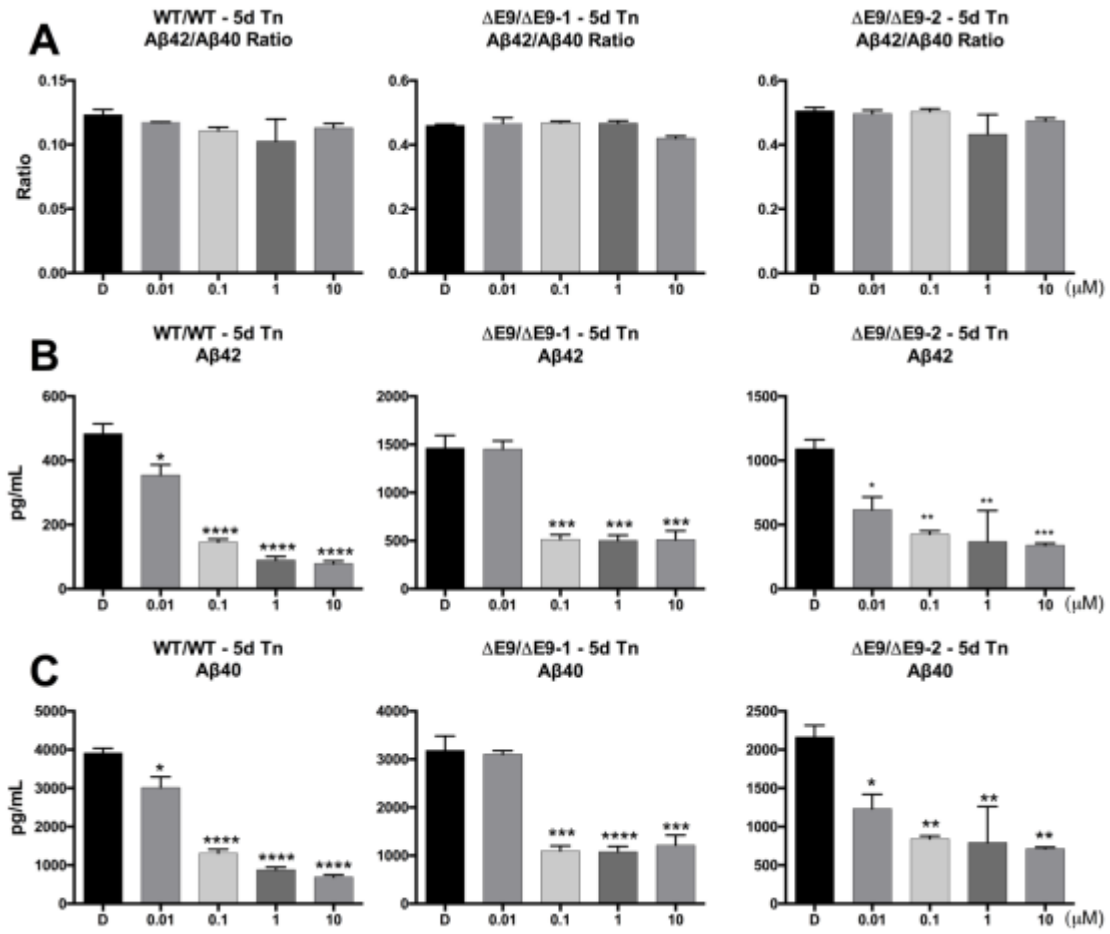

Figure 8. Extended treatment of neurons with tunicamycin does not affect Aβ42/Aβ40 ratio, but does decrease both Aβ42 and Aβ40. Secreted Aβ42/Aβ40 ratio (A), Aβ42 (B), and Aβ40 (C) were measured from wild-type and PS1-ΔE9 mutants treated with increasing concentrations of tunicamycin (Tn) for five days. Bars represent measurements from one experiment normalized to total protein concentration. Error bars represent SEM from three biological replicates per experiment. Additional experiments were repeated and showed similar results, but could not normalize to total protein (data not shown). Statistics performed via One-way ANOVA. *p<0.05, **p<0.01, ***p<0.001, ****p < 0.0001.

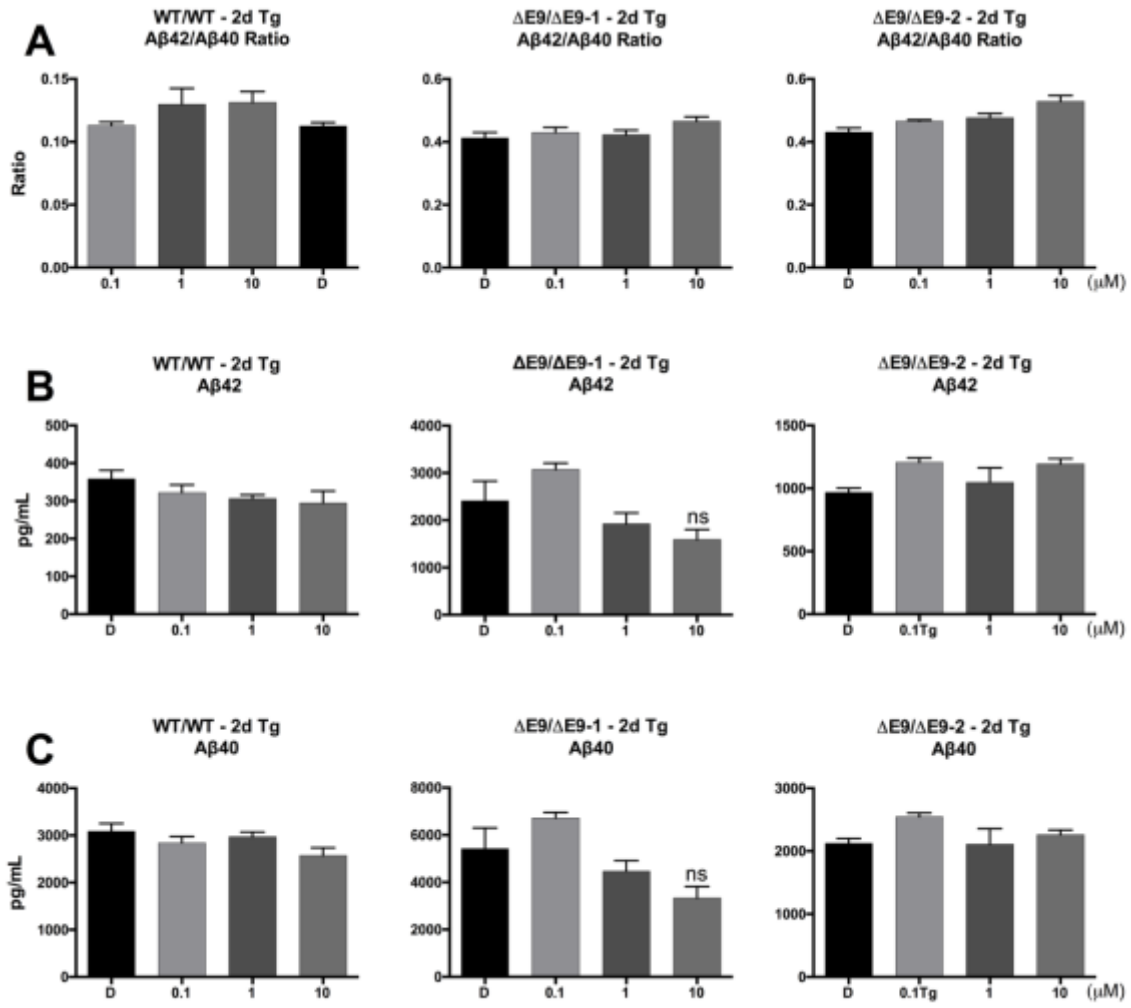

Figure 9. Thapsigargin-induced ER stress does not change the Aβ42/Aβ40 ratio. Secreted Aβ42/Aβ40 ratio (A), Aβ42 (B), and Aβ40 (C) were measured from wild-type and PS1-ΔE9 mutants treated with increasing concentrations of thapsigargin (Tg) for two days. Bars represent measurements from two independent experiments and normalized to total protein concentration. Error bars represent SEM from three biological replicates per experiment. Additional experiments were repeated and showed similar results, but could not normalize to total protein (data not shown). Statistics performed via One-way ANOVA.

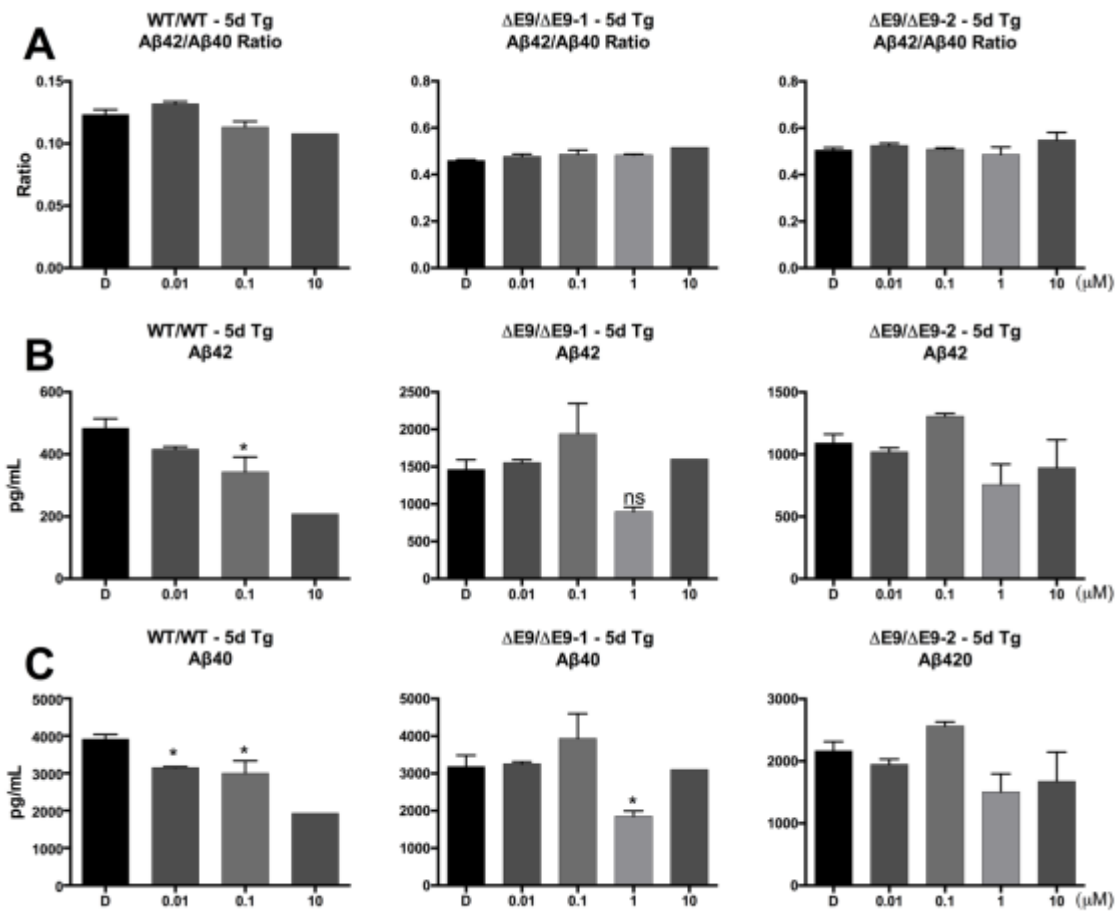

Figure 10. Extended treatment of neurons with thapsigargin does not affect the Aβ42/Aβ40 ratio in wild-type or PS1-ΔE9 neurons, but decreases Aβ42 and Aβ40 in wild-type neurons. Secreted Aβ42/Aβ40 ratio (A), Aβ42 (B), and Aβ40 (C) were measured from wild-type and PS1-ΔE9 mutants treated with increasing concentrations of thapsigargin (Tg) for five days. Bars represent measurements from one experiment normalized to total protein concentration. Error bars represent SEM from three biological replicates per experiment. Additional experiments were repeated and showed similar results, but could not normalize to total protein (data not shown). No value shown for 1 μM thapsigargin in WT/WT due to an error in the measurements. Statistics performed via One-way ANOVA. *p < 0.05, **p<0.01, ***p<0.001, ****p<0.0001.

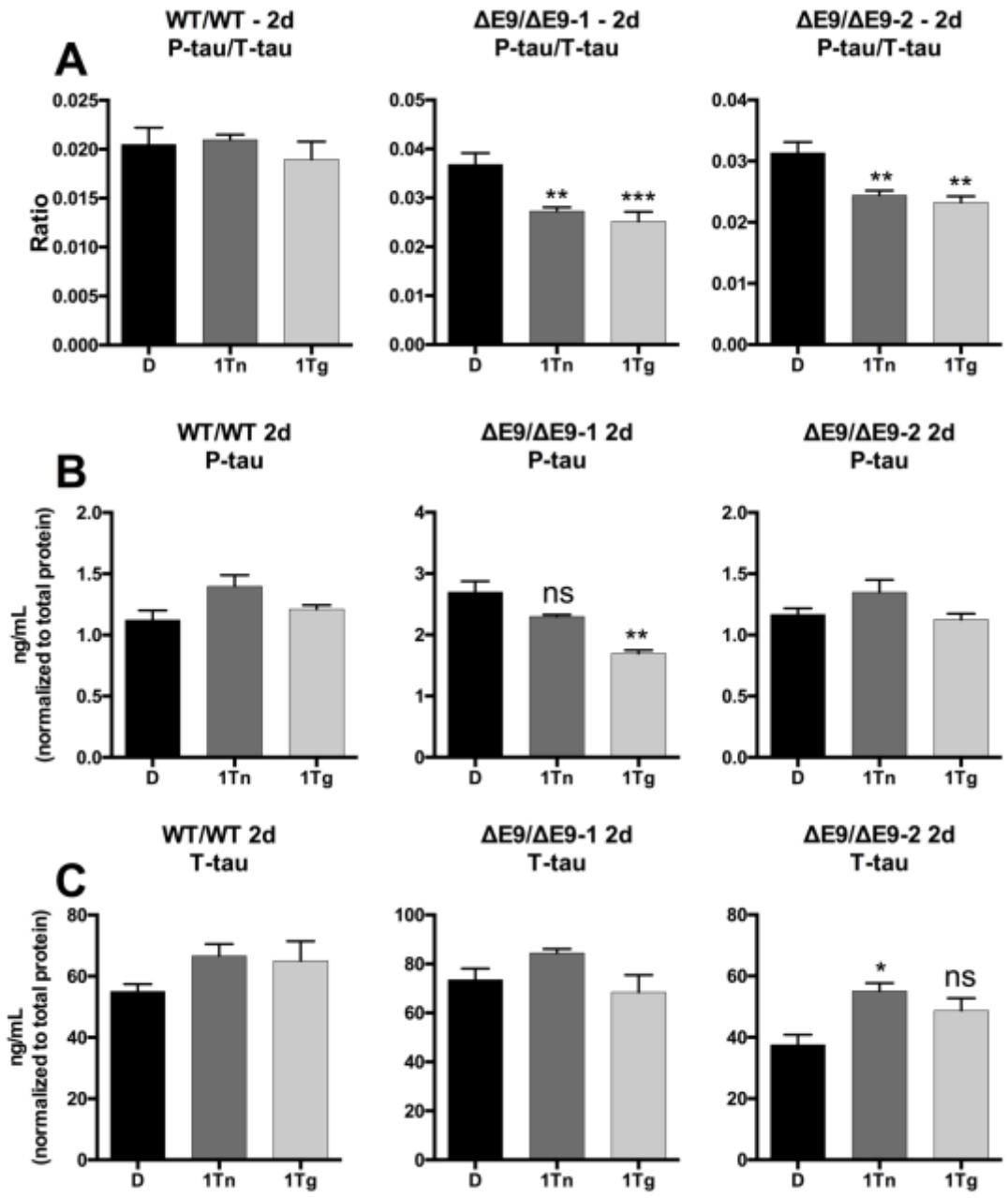

Figure 11. ER stress induced for two days reduces p-tau/t-tau ratio in PS1-ΔE9 neurons. Total tau (T-tau) and phosphorylated tau (P-tau) were measured in wild-type and PS1-ΔE9 neurons after treatment with 1 μM tunicamycin (Tn) or 1 μM thapsigargin (Tg) for two days. Bars represent mean of one experiment. Error bars represent SEM from three biological replicates. *p < 0.05, **p<0.01, ***p<0.001, ****p<0.0001 by One-way ANOVA.

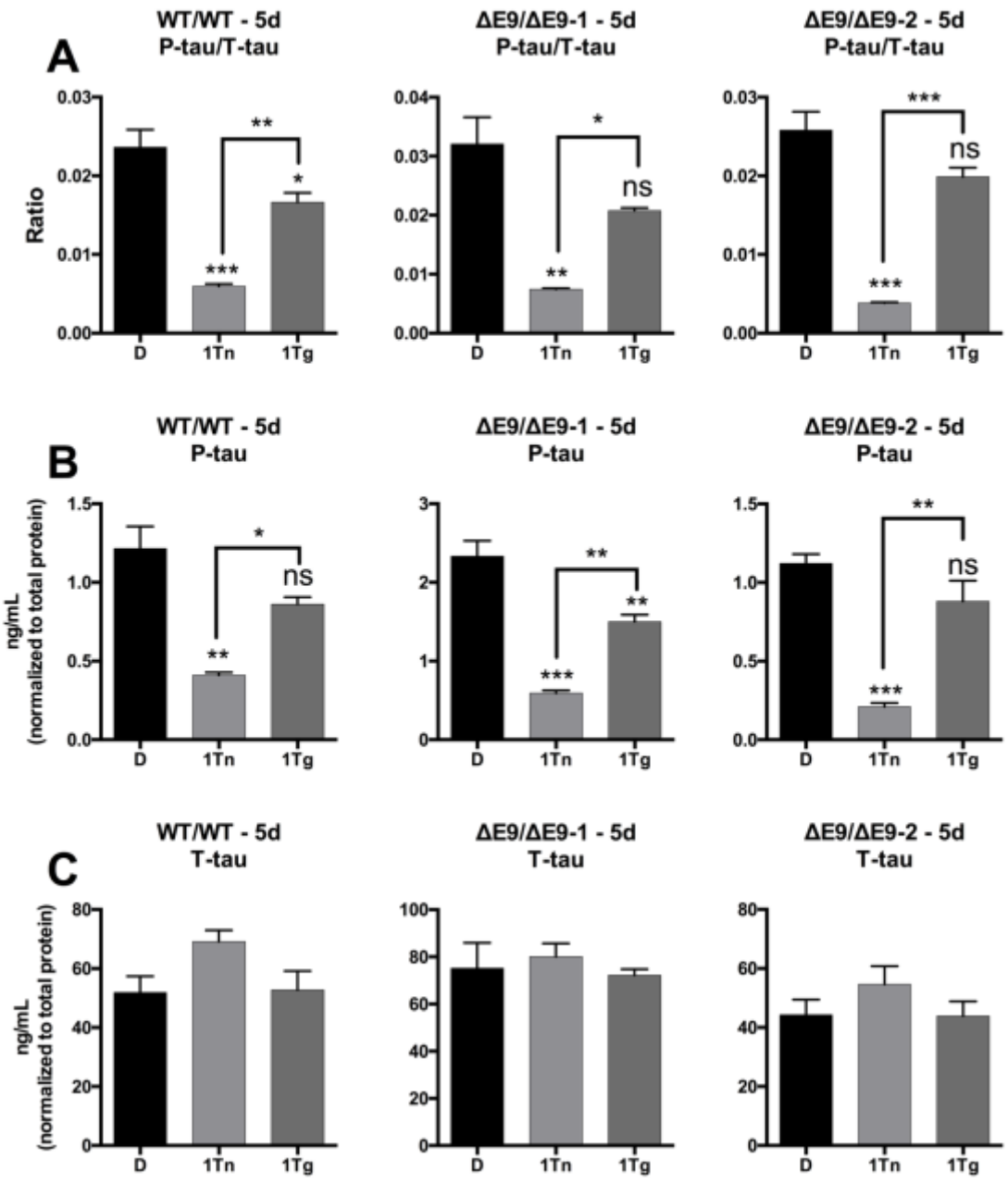

Figure 12. Prolonged induction of ER stress by tunicamycin reduces P-tau/T-tau ratio by decreasing P-tau. Total tau (T-tau) and phosphorylated tau (P-tau) were measured in wild-type and PS1-ΔE9 neurons after treatment with 1 μM tunicamycin (Tn) or 1 μM thapsigargin (Tg) for five days. Bars represent mean of one experiment. Error bars represent SEM from three biological replicates. *p < 0.05, **p<0.01, ***p<0.001, ****p<0.0001 by One-way ANOVA.

DISCUSSION

In the present study, we have demonstrated that NSCs are more sensitive to ER stress-induced cell death than neurons, that an FAD PS1-ΔE9 mutation in NSCs and neurons alters cellular viability in response to ER stress, and the same mutation in neurons changes levels of ER stress gene expression before and after ER stress is induced. Additionally, we showed that inducing ER stress with tunicamycin or thapsigargin does not affect the Aβ42/Aβ42 ratio in human neurons. This is due to reductions in both Aβ42 and Aβ40 levels, and is independent of the PS1-ΔE9 mutation. Our results also show that tunicamycin- and thapsigargin-induced ER stress reduces the P-tau/T-tau ratio in wild type and PS1-ΔE9 neurons by reducing P-tau levels.

Previous experiments studying the relationship between ER stress and presenilin mutations, Aβ, or P-tau have typically used non-neuronal cell lines and mouse models (Dorner et al., 1990; Drummond and Wisniewski, 2017; Gerakis et al., 2016; Takahashi et al., 2009). However, Alzheimer's is a neurodegenerative disease where Aβ plaques, neurofibrillary tangles, and cell death all occur in neurons, with astrocytes, microglia, and other neural cells implicated in disease progression as well. Thus, it is important to use the relevant human cell type in studying AD to be able to make accurate conclusions. Prior research looking at the relationship between PS1 mutations and ER stress has yielded controversial results, with some researchers claiming that PS1 mutations suppress the expression of *BiP* in response to ER stress (Katayama et al., 1999), or that presenilin is required for proper UPR function (Katayama et al., 2001; Niwa et al., 1999; Yasuda et al., 2002). However, other groups claim that mutations in PS1 have no effect on the UPR (Piccini et al., 2004; Sato et al., 2000). We believe one of the reasons for the controversy

surrounding presenilin mutations and ER stress is due to the use of different, non-neuronal cell types in conjunction with overexpression of the presenilin mutations.

From our studies using hiPSC-derived neurons and NSCs containing a representative FAD PS1-ΔE9 mutation, we observed greater sensitivity to tunicamycin in NSCs (Figure 3A) and neurons (Figure 6A). This is similar to what Katayama et al., 1999 observed after using tunicamycin to induce ER stress in neuroblastoma cells transfected with the PS1-ΔE9 mutation. When we treated wild type and PS1-ΔE9 neurons with thapsigargin, however, we observed opposite results, where the wild type neurons were more sensitive than the PS1-ΔE9 neurons were (Figure 7B). This suggests that neurons expressing the PS1-ΔE9 mutation may not be as sensitive to ER stress induced by thapsigargin as the wild type line. The ER is a major calcium storage organelle in mammalian cells, and disruptions in ER calcium homeostasis can lead to ER stress. Although we did not expect these results, we believe that it fits with what we currently know about presenilin proteins and their involvement with ER calcium homeostasis. Thapsigargin induces ER stress by inhibiting SERCA, which causes depletion of ER Ca^{2+} and excess Ca^{2+} buildup in the cytosol. Presenilin proteins themselves act as Ca^{2+} leak channels (Bezprozvanny and Mattson, 2008; Tu et al., 2006; Zhang et al., 2010), and so homeostasis is achieved with a balance of SERCA pump activity and PS1 leak activity. While most FAD mutations cause a loss of function in ER Ca^{2+} leak activity, resulting in accumulation of Ca^{2+} in the ER lumen (Tu et al., 2006), the PS1-ΔE9 mutant acts as a gain of function mutation in ER Ca^{2+} leak activity, leading to excessive Ca^{2+} present in the cytosol of the cell and a partially Ca^{2+}-depleted ER (Tu et al., 2006). Preliminary Ca^{2+} experiments performed in the lab have recapitulated these results, confirming that the

PS1-ΔE9 mutation present in our neurons results in increased cytosolic Ca^{2+} levels and decreased ER Ca^{2+} levels (Chaves R. S., unpublished data). This may help to explain our viability results in response to thapsigargin treatment: since the PS1-ΔE9 mutation results in an already Ca^{2+}-depleted ER, thapsigargin has reduced effectiveness because there is less Ca^{2+} present in the ER from the beginning. To further investigate whether the PS1-ΔE9 mutation confers resistance to Ca^{2+}-mediated ER stress, we would use a different compound that also depletes ER Ca^{2+} levels and increases cytosolic Ca^{2+} levels, such as calcium ionophore A23187.

This hypothesis was further tested when we measured relative levels of gene expression after thapsigargin treatment. We observed a greater increase in *BiP* and *CHOP* expression in the wild type neurons compared to the PS1-ΔE9 neurons with thapsigargin treatment (Figure 8C; left, right) but not with tunicamycin treatment (Figure 8B; left, right). When we looked at spliced *XBP1* levels, we saw that the levels of spliced *XBP1* in one mutant were elevated compared to wild type, while the levels of spliced *XBP1* in the other mutant were not statistically different compared to wild type after tunicamycin treatment (Figure 8B, center). Our results contrast with the findings of Katayama et al., 1999 because we did not see a suppression of the UPR in neurons bearing the PS1-ΔE9 mutation after tunicamycin treatment; instead, we saw suppression of *BiP* and *CHOP* expression in the PS1-ΔE9 mutants in response to thapsigargin treatment. Our results show that *BiP* and *CHOP* expression in response to thapsigargin-induced ER stress is suppressed by the PS1-ΔE9 mutation, whereas *XBP1* splicing and ER stress gene expression in response to tunicamycin is not consistently altered by the presence of the PS1-ΔE9 mutation.

We hypothesized that the differences observed between the two PS1-ΔE9 mutants—which were generated from an isogenic background— may have arisen from variability that occurs during genome-editing of subcloned iPSCs. Woodruff et al., 2013 had addressed this concern by performing whole-exome sequencing on the TALEN-modified iPSC lines and the parental iPSC lines. They showed that the wild type control line had zero off-target mutations, and the PS1-ΔE9 mutants contained one to two unique mutations (Woodruff et al., 2013). One of the mutations in just one of the homozygous PS1-ΔE9 lines was an arginine to histidine substitution in the s*ignal transducer and activator of transcription 3 (STAT3)* gene, which plays a role in the expression of various genes in response to stimuli, and has roles in many processes such as cell growth and apoptosis. This may help to explain the differences in viability seen in the two mutant lines used in this study. Another possible point of difference between the two PS1-ΔE9 mutants that we cannot rule out is the potential for mutations in the introns of the mutants' genome. Woodruff et al. performed whole-exome sequencing to look for protein-coding mutations, introns have numerous functions in transcription initiation and termination, and transcription regulation and alternative splicing, to name a few (Carmel and Chorev, 2012) that may potentially impact the cells' response to ER stress.

Previous studies examining the effects of amyloid-β oligomers on ER stress have found that the addition of Aβ42 to culture medium induces ER stress and apoptosis (Chafekar et al., 2007; Lee et al., 2010; Multhaup et al., 2015). Additional research showed that tunicamycin-induced ER stress lead to elevated Aβ42 production in fibroblasts (Piccini et al., 2004)and in retinal ganglion cells (RGC-5) (Liu et al., 2014). Because these studies used non-neuronal cells, we wanted to see whether we would

observe similar results in human neurons. We initially hypothesized that the treating the PS1-ΔE9 neurons with tunicamycin would result in even higher Aβ42 levels and thus a higher Aβ42/Aβ40 ratio after tunicamycin treatment. This was not the case, however, as we observed reductions in both Aβ42 and Aβ40 levels with tunicamycin treatment for two and five days. With thapsigargin treatment, we observed slight decreases in Aβ42 and Aβ40 after five days, primarily in the wild type neurons, and no changes in Aβ42 and Aβ40 in the PS1-ΔE9 neurons. One study has shown that ER stress induces polyubiquitination of APP, targeting it for degradation via the ubiquitin proteasome system (Jung et al., 2015). Although Jung et al., 2015 used Chinese hamster ovary cells and used a different ER stress inducer, this may help shed light on the reduction of both Aβ42 and Aβ40 in response to tunicamycin-induced ER stress in our system. Another potential explanation could be due to how tunicamycin induces ER stress. Tunicamycin inhibits N-glycosylation of proteins, which has significant ramifications for how APP is transported and processed within the cell. However, we cannot rule out the possibility that the reduction in Aβ42 and Aβ40 may be due to cell death upon treatment with tunicamycin, because we observed almost a 50% reduction in neuron viability with tunicamycin treatment for five days.

Research on the relationship between ER stress and tau phosphorylation has indicated that ER stress increases tau phosphorylation (Resende et al., 2008; Rueli et al., 2017). We observed the opposite in our neurons, with tunicamycin-induced ER stress significantly reducing the P-tau/T-tau ratio in only the PS1-ΔE9 mutants after two days, and reducting the ratio in wild-type and PS1-ΔE9 neurons after five days. These results suggest that the P-tau/T-tau ratio in PS1-ΔE9 mutants are more sensitive to changes from

tunicamycin-induced ER stress. However, because these results come from a single experiment, albeit performed with biological triplicates, more experiments are needed to strengthen our results. Additionally, although we observed a time-dependent decrease in P-tau, we do not know if we would observe a dose-dependent decrease (or increase) in P-tau since our results only show one concentration of tunicamycin and thapsigargin used. Finally, we cannot rule out the possibility that the reduction in P-tau seen after five days may have been due to cell death caused by the drug treatments.

Overall, our results suggest that the FAD PS1-ΔE9 mutation expressed in human neurons sensitizes them to tunicamycin-induced ER stress, while at the same time confers resistance to thapsigargin-induced ER stress. Our results also show that the PS1-ΔE9 mutation suppresses *BiP* and *CHOP* expression in response to thapsigargin, but gene expression in response to tunicamycin is not genome-dependent. Contrary to prior research in the field, our results suggest that tunicamycin-induced ER stress may decrease Aβ42, Aβ40, and P-tau levels, suggesting that either ER stress or inhibiting N-glycosylation is "rescuing" the AD phenotype.

MATERIALS AND METHODS

Cell Lines

The PS1-ΔE9 NSCs used in the present study were previously generated by members of the lab. Briefly, they cultured hiPSCs on an irradiated mouse embryonic fibroblast (MEF) feeder layer generated in-house. hiPSC genomes were edited using TAL effector nuclease (TALEN) technology to introduce the FAD-associated *PSEN1*-ΔE9 mutation. (Woodruff et al., 2013)

Cell Culture

NSCs were grown and maintained in Dulbecco's Modified Eagle Medium/Nutrient Mixture F-12 (DMEM/F12; ThermoFisher) supplemented with B-27, N-2 (Life Technologies), penicillin-streptomycin (100 U/mL, Life Technologies) and fibroblast growth factor (FGF; EMD Millipore, 20 ng/mL). Media was changed every other day. When grown to ~90% confluency, NSCs were dissociated with Accutase (Innovative Cell Technologies) and expanded onto poly-L-ornithine hydrobromide- (PLO, 20 µg/ml) and laminin- (5 µg/mL) coated 10 cm plates and grown to confluency, at which point FGF was removed from the media. The medium was changed twice per week and the cells were allowed to differentiate for 21 days. After the three-week differentiation, neurons were dissociated using Accutase and Accumax (Innovative Cell Technologies) and then passed through a 100 µm filter before plating onto PLO/laminin-coated plates in NSC media containing 0.5 mM dbCAMP (Sigma), 20 ng/µl brain-derived neurotrophic factor (BDNF; Peprotech), and 20 ng/µl glial cell line-derived neurotrophic factor (GDNF; Peprotech). Cultures were incubated at 37°C in a 95% air/5% CO_2 humidified atmosphere. Cells were then treated with tunicamycin (Sigma), thapsigargin (Sigma), MG132 (EMD Millipore), or staurosporine (Sigma). These

compounds were solubilized in DMSO to make stock concentrations. 0.01% DMSO was used as a vehicle control for studies with these compounds.

Cell Viability Assay

Cell viability was measured via the CellTiter 96® AQueous One Solution Cell Proliferation Assay (Promega). After each treatment, the assay was added to the culture medium and cells were incubated at 37°C. After incubation, absorption was measured on a microplate reader (Infinite 200, Tecan Trading AG, Switzerland) at 490 nm, with a reference wavelength of 675 nm to subtract background.

RT-qPCR

To compare RNA levels between samples, RNA was isolated from cells using the RNeasy Mini Kit (Qiagen), purified with the Turbo DNA-free Kit (ThermoFisher), and reverse transcribed using the SuperScript® First-Strand Synthesis System (ThermoFisher). qPCR was performed using FastStart Universal SYBR Green Master Mix (Roche) with the primers listed in Table 1, and analyzed on an Applied Biosystems 7300 Real Time PCR System. Relative RNA levels were normalized to the housekeeping gene *Ribosomal Protein L27* (*RPL27*). The PCR conditions were as follows: 50°C for 2 min for prevention of carryover contamination; 95°C for 10 min to activate the FastStart Taq DNA polymerase; 45 cycles of 95°C for 15s, 58°C for 18s, and 72°C for 30s for annealing, extension, and fluorescence reading; and one cycle of 95°C for 15s and 60°C for 1 min for amplification and real-time analysis.

Amyloid-β, pTau/total tau measurements

Three-week differentiated neurons were plated at 2 x 10^5 per well of a 96-well plate. Cells were cultured for an additional two weeks with no media change. On the 14th

day, full media change was performed, along with any drug treatments. Cells were cultured for an additional two to five days. Amyloid-β was measured with V-PLEX Aβ Peptide Panel 1 (6E10) Kit (Meso Scale Discovery). pTau/total tau was measured with a Phospho (Thr231)/Total Tau Kit (Meso Scale Discovery). Values were normalized to total protein levels determined by BCA assay (ThermoFisher).

Statistics

For each graph, statistics were performed by using either a one-way ANOVA with Dunnet correction for multiple comparisons, or by two-tailed Student's t-test using GraphPad Prism 6. The data were presented as the mean ± SEM.

Table 1. Primers used for qPCR

Primers	
Gene	**Primer Sequence**
RPL27	F – ACATTGATGATGGCACCTCAG R – CCAAGGGGATATCCACAGAGT
Non-spliced *XBP-1*	F – ACTCAGACTACGTGCACCTCT R – GCTGGCAGGCTCTGGGGAAG
Spliced *XBP-1*	F – TGCTGAGTCCGCAGCAGGTG R – GCTGGCAGGCTCTGGGGAAG
BiP	F – CAAAGACATTTGCTCCTGAAGA R – TTGCCCGTCTTCTTTTTGTA
CHOP	F – CAGAGCTGGAACCTGAGGAG R – CAGTGTCCCGAAGGAGAAAG

REFERENCES

Alonso, A.C., Zaidi, T., Grundke-Iqbal, I., and Iqbal, K. (1994). Role of abnormally phosphorylated tau in the breakdown of microtubules in Alzheimer disease. Proc. Natl. Acad. Sci. U. S. A. *91*, 5562–5566.

Alzheimer's Association Younger/Early Onset | Alzheimer's Association.

Barnes, D.E., and Yaffe, K. (2011). The projected effect of risk factor reduction on Alzheimer's disease prevalence. Lancet Neurol. *10*, 819–828.

Bekris, L.M., Yu, C.-E., Bird, T.D., and Tsuang, D.W. (2010). Review Article: Genetics of Alzheimer Disease. J. Geriatr. Psychiatry Neurol. *23*, 213–227.

Bezprozvanny, I., and Mattson, M.P. (2008). Neuronal calcium mishandling and the pathogenesis of Alzheimer's disease. Trends Neurosci. *31*, 454–463.

Carmel, L., and Chorev, M. (2012). The Function of Introns. Front. Genet. *3*.

Cornejo, V.H., and Hetz, C. (2013). The unfolded protein response in Alzheimer's disease. Semin. Immunopathol. *35*, 277–292.

Dong, J., Qin, W., Wei, C., Tang, Y., Wang, Q., and Jia, J. (2017). A Novel PSEN1 K311R Mutation Discovered in Chinese Families with Late-Onset Alzheimer's Disease Affects Amyloid-β Production and Tau Phosphorylation. J. Alzheimers Dis. *Preprint*, 1–11.

Dorner, A.J., Wasley, L.C., Raney, P., Haugejorden, S., Green, M., and Kaufman, R.J. (1990). The stress response in Chinese hamster ovary cells. Regulation of ERp72 and protein disulfide isomerase expression and secretion. J. Biol. Chem. *265*, 22029–22034.

Drummond, E., and Wisniewski, T. (2017). Alzheimer's disease: experimental models and reality. Acta Neuropathol. (Berl.) *133*, 155–175.

Forman, M.S., Lee, V.M.-Y., and Trojanowski, J.Q. (2003). "Unfolding" pathways in neurodegenerative disease. Trends Neurosci. *26*, 407–410.

Gerakis, Y., Dunys, J., Bauer, C., and Checler, F. (2016). Aβ42 oligomers modulate β-secretase through an XBP-1s-dependent pathway involving HRD1. Sci. Rep. *6*.

Gething, M.-J. (1999). Role and regulation of the ER chaperone BiP. Semin. Cell Dev. Biol. *10*, 465–472.

Grundke-Iqbal, I., Iqbal, K., Tung, Y.C., Quinlan, M., Wisniewski, H.M., and Binder, L.I. (1986). Abnormal phosphorylation of the microtubule-associated protein tau (tau) in Alzheimer cytoskeletal pathology. Proc. Natl. Acad. Sci. U. S. A. *83*, 4913–4917.

Haapasalo, A., and Kovacs, D.M. (2011). The Many Substrates of Presenilin/γ-Secretase. J. Alzheimers Dis. *25*, 3–28.

Hardy, J., and Allsop, D. (1991). Amyloid deposition as the central event in the aetiology of Alzheimer's disease. Trends Pharmacol. Sci. *12*, 383–388.

Hardy, J.A., and Higgins, G.A. (1992). Alzheimer's disease: the amyloid cascade hypothesis. Science *256*, 184–185.

Hoozemans, J.J.M., Veerhuis, R., Haastert, E.S.V., Rozemuller, J.M., Baas, F., Eikelenboom, P., and Scheper, W. (2005). The unfolded protein response is activated in Alzheimer's disease. Acta Neuropathol. (Berl.) *110*, 165–172.

Hoozemans, J.J.M., van Haastert, E.S., Nijholt, D.A.T., Rozemuller, A.J.M., Eikelenboom, P., and Scheper, W. (2009). The Unfolded Protein Response Is Activated in Pretangle Neurons in Alzheimer's Disease Hippocampus. Am. J. Pathol. *174*, 1241–1251.

Jäger, R., Bertrand, M.J.M., Gorman, A.M., Vandenabeele, P., and Samali, A. (2012). The unfolded protein response at the crossroads of cellular life and death during endoplasmic reticulum stress. Biol. Cell *104*, 259–270.

Janus, C., Chishti, M.A., and Westaway, D. (2000). Transgenic mouse models of Alzheimer's disease. Biochim. Biophys. Acta BBA - Mol. Basis Dis. *1502*, 63–75.

Katayama, T., Imaizumi, K., Sato, N., Miyoshi, K., Kudo, T., Hitomi, J., Morihara, T., Yoneda, T., Gomi, F., Mori, Y., Nakano, Y., Takeda, J., Tsuda, T., Itoyama, Y., Murayama, O., Takashima, A., St George-Hyslop, P., Takeda, M., and Tohyama, M. (1999). Presenilin-1 mutations downregulate the signalling pathway of the unfolded-protein response. Nat. Cell Biol. *1*, 479–485.

Katayama, T., Imaizumi, K., Honda, A., Yoneda, T., Kudo, T., Takeda, M., Mori, K., Rozmahel, R., Fraser, P., George-Hyslop, P.S., and Tohyama, M. (2001). Disturbed Activation of Endoplasmic Reticulum Stress Transducers by Familial Alzheimer's Disease-linked Presenilin-1 Mutations. J. Biol. Chem. *276*, 43446–43454.

Katayama, T., Imaizumi, K., Manabe, T., Hitomi, J., Kudo, T., and Tohyama, M. (2004). Induction of neuronal death by ER stress in Alzheimer's disease. J. Chem. Neuroanat. *28*, 67–78.

Kelleher, R.J., and Shen, J. (2017). Presenilin-1 mutations and Alzheimer's disease. Proc. Natl. Acad. Sci. *114*, 629–631.

Kim, J., Chakrabarty, P., Hanna, A., March, A., Dickson, D.W., Borchelt, D.R., Golde, T., and Janus, C. (2013). Normal cognition in transgenic BRI2-Aβ mice. Mol. Neurodegener. *8*, 15.

Kosik, K.S., Joachim, C.L., and Selkoe, D.J. (1986). Microtubule-associated protein tau (tau) is a major antigenic component of paired helical filaments in Alzheimer disease. Proc. Natl. Acad. Sci. U. S. A. *83*, 4044–4048.

Lee, D.Y., Lee, K.-S., Lee, H.J., Kim, D.H., Noh, Y.H., Yu, K., Jung, H.-Y., Lee, S.H., Lee, J.Y., Youn, Y.C., Jeong, Y., Kim, D.K., Lee, W.B., and Kim, S.S. (2010). Activation of PERK Signaling Attenuates Aβ-Mediated ER Stress. PLOS ONE *5*, e10489.

Lin, J.H., Walter, P., and Yen, T.S.B. (2008). Endoplasmic Reticulum Stress in Disease Pathogenesis. Annu. Rev. Pathol. Mech. Dis. *3*, 399–425.

Luedecke, D., Becktepe, J.S., Lehmbeck, J.T., Finckh, U., Yamamoto, R., Jahn, H., and Boelmans, K. (2014). A novel presenilin 1 mutation (Ala275Val) as cause of early-onset familial Alzheimer disease. Neurosci. Lett. *566*, 115–119.

Merksamer, P.I., and Papa, F.R. (2010). The UPR and cell fate at a glance. J Cell Sci *123*, 1003–1006.

Naidoo, N., and Brown, M. (2012). The endoplasmic reticulum stress response in aging and age-related diseases. Front. Physiol. *3*.

Niwa, M., Sidrauski, C., Kaufman, R.J., and Walter, P. (1999). A Role for Presenilin-1 in Nuclear Accumulation of Ire1 Fragments and Induction of the Mammalian Unfolded Protein Response. Cell *99*, 691–702.

Oslowski, C.M., and Urano, F. (2011). Measuring ER stress and the unfolded protein response using mammalian tissue culture system. Methods Enzymol. *490*, 71–92.

Pereira, C.M.F. (2013). Crosstalk between Endoplasmic Reticulum Stress and Protein Misfolding in Neurodegenerative Diseases. Int. Sch. Res. Not. *2013*, e256404.

Piccini, A., Fassio, A., Pasqualetto, E., Vitali, A., Borghi, R., Palmieri, D., Nacmias, B., Sorbi, S., Sitia, R., and Tabaton, M. (2004a). Fibroblasts from FAD-linked presenilin 1 mutations display a normal unfolded protein response but overproduce Aβ42 in response to tunicamycin. Neurobiol. Dis. *15*, 380–386.

Piccini, A., Fassio, A., Pasqualetto, E., Vitali, A., Borghi, R., Palmieri, D., Nacmias, B., Sorbi, S., Sitia, R., and Tabaton, M. (2004b). Fibroblasts from FAD-linked presenilin 1 mutations display a normal unfolded protein response but overproduce Aβ42 in response to tunicamycin. Neurobiol. Dis. *15*, 380–386.

Placido, A.I., Pereira, C.M.F., Duarte, A.I., Candeias, E., Correia, S.C., Santos, R.X., Carvalho, C., Cardoso, S., Oliveira, C.R., and Moreira, P.I. (2014). The role of endoplasmic reticulum in amyloid precursor protein processing and trafficking: Implications for Alzheimer's disease. Biochim. Biophys. Acta BBA - Mol. Basis Dis. *1842*, 1444–1453.

Resende, R., Ferreiro, E., Pereira, C., and Oliveira, C.R. (2008). ER stress is involved in Aβ-induced GSK-3β activation and tau phosphorylation. J. Neurosci. Res. *86*, 2091–2099.

Rodríguez-Martín, T., Cuchillo-Ibáñez, I., Noble, W., Nyenya, F., Anderton, B.H., and Hanger, D.P. (2013). Tau phosphorylation affects its axonal transport and degradation. Neurobiol. Aging *34*, 2146–2157.

Sato, N., Urano, F., Yoon Leem, J., Kim, S.-H., Li, M., Donoviel, D., Bernstein, A., Lee, A.S., Ron, D., Veselits, M.L., Sisodia, S.S., and Thinakaran, G. (2000). Upregulation of BiP and CHOP by the unfolded-protein response is independent of presenilin expression. Nat. Cell Biol. *2*, 863–870.

Scheuner, D., Eckman, C., Jensen, M., Song, X., Citron, M., Suzuki, N., Bird, T.D., Hardy, J., Hutton, M., Kukull, W., Larson, E., Levy-Lahad, L., Viitanen, M., Peskind, E., Poorkaj, P., Schellenberg, G., Tanzi, R., Wasco, W., Lannfelt, L., Selkoe, D., and Younkin, S. (1996). Secreted amyloid β–protein similar to that in the senile plaques of Alzheimer's disease is increased in vivo by the presenilin 1 and 2 and APP mutations linked to familial Alzheimer's disease. Nat. Med. *2*, 864–870.

Shepherd, C., McCann, H., and Halliday, G.M. (2009). Variations in the neuropathology of familial Alzheimer's disease. Acta Neuropathol. (Berl.) *118*, 37–52.

Song, L., Sarno, P.D., and Jope, R.S. (2002). Central Role of Glycogen Synthase Kinase-3β in Endoplasmic Reticulum Stress-induced Caspase-3 Activation. J. Biol. Chem. *277*, 44701–44708.

Strobel, G. What Is Early Onset Familial Alzheimer Disease (eFAD)? | ALZFORUM.

Sun, L., Zhou, R., Yang, G., and Shi, Y. (2017). Analysis of 138 pathogenic mutations in presenilin-1 on the in vitro production of Aβ42 and Aβ40 peptides by γ-secretase. Proc. Natl. Acad. Sci. *114*, E476–E485.

Tabas, I., and Ron, D. (2011). Integrating the mechanisms of apoptosis induced by endoplasmic reticulum stress. Nat. Cell Biol. *13*, 184–190.

Takahashi, K., Tanabe, K., Ohnuki, M., Narita, M., Ichisaka, T., Tomoda, K., and Yamanaka, S. (2007). Induction of Pluripotent Stem Cells from Adult Human Fibroblasts by Defined Factors. Cell *131*, 861–872.

Takahashi, K., Niidome, T., Akaike, A., Kihara, T., and Sugimoto, H. (2009). Amyloid precursor protein promotes endoplasmic reticulum stress-induced cell death via C/EBP homologous protein-mediated pathway. J. Neurochem. *109*, 1324–1337.

Taylor, J.P., Hardy, J., and Fischbeck, K.H. (2002). Toxic Proteins in Neurodegenerative Disease. Science *296*, 1991–1995.

Tu, H., Nelson, O., Bezprozvanny, A., Wang, Z., Lee, S.-F., Hao, Y.-H., Serneels, L., De Strooper, B., Yu, G., and Bezprozvanny, I. (2006). Presenilins Form ER Ca2+ Leak Channels, a Function Disrupted by Familial Alzheimer's Disease-Linked Mutations. Cell *126*, 981–993.

Walter, P., and Ron, D. (2011). The Unfolded Protein Response: From Stress Pathway to Homeostatic Regulation. Science *334*, 1081–1086.

Weingarten, M.D., Lockwood, A.H., Hwo, S.Y., and Kirschner, M.W. (1975). A protein factor essential for microtubule assembly. Proc. Natl. Acad. Sci. U. S. A. *72*, 1858–1862.

Woodruff, G., Young, J.E., Martinez, F.J., Buen, F., Gore, A., Kinaga, J., Li, Z., Yuan, S.H., Zhang, K., and Goldstein, L.S.B. (2013). The Presenilin-1 ΔE9 Mutation Results in Reduced γ-Secretase Activity, but Not Total Loss of PS1 Function, in Isogenic Human Stem Cells. Cell Rep. *5*, 974–985.

Yasuda, Y., Kudo, T., Katayama, T., Imaizumi, K., Yatera, M., Okochi, M., Yamamori, H., Matsumoto, N., Kida, T., Fukumori, A., Okumura, M., Tohyama, M., and Takeda, M. (2002). FAD-linked presenilin-1 mutants impede translation regulation under ER stress. Biochem. Biophys. Res. Commun. *296*, 313–318.